Fabrication of Chemical Vapor Deposition (CVD) Setup

&

Preparation of Copper Oxide (CuO) -CdX (X= Se, S) Nanoparticles Decorated Core-Shell Heterostructure

Bamadev Das

Department of Physics & Astronomy

National Institute of Technology Rourkela

Rourkela-769008, Odisha, India

Fabrication of Chemical Vapor Deposition (CVD) Setup & Preparation of Copper Oxide (CuO)-CdX (X= Se, S) Nanoparticles Decorated Core-Shell Heterostructure

Thesis submitted in partial fulfillment
of the requirements for the degree of

Master in Technology (Research)

In

Physics

By

Bamadev Das
(Roll No.-612ph301)

Under The Supervision of

Dr. Pitamber Mahanandia

Assistant Professor,

Department of Physics & Astronomy, NIT Rourkela

Department of Physics & Astronomy

National Institute of Technology Rourkela

Rourkela-769008, Odisha, India

I would like to dedicate my thesis to my Grandfather, late Baidyanath Das, Late Baisnaba Sendhamahapatra, my loving parents Mr. Ramakanta Das, Mrs. Bhagabati Das & my loving brother Amit K. Das

Department of Physics & Astronomy
National Institute of Technology Rourkela
Rourkela-769008, Odisha, India.

Dr. Pitamber Mahanandia

Assistant Professor

Department of Physics & Astronomy

Certificate

This is to certify that, the work in the report entitled **"Fabrication of Chemical Vapor Deposition (CVD) Setup & Preparation of Copper Oxide (CuO)-CdX (X= Se, S) Nanoparticles Decorated Core-Shell Heterostructure"** by **Bamadev Das,** in partial fulfillment of Master of Technology (Research) degree in **PHYSICS** at the National Institute of Technology, Rourkela, Odisha is an authentic work carried out by him under my supervision and guidance. The work is new and satisfactory to the best my knowledge.

Dr. Pitamber Mahanandia

Department of Physics & Astronomy
National Institute of Technology Rourkela
Rourkela-769008, Odisha, India.

Bamadev Das

612ph301

Declaration

I hereby declare that the project work entitled "**Fabrication of Chemical Vapor Deposition (CVD) Setup & Preparation of Copper Oxide (CuO)-CdX (X= Se, S) Nanoparticles Decorated Core-Shell Heterostructure**" submitted to the NIT, Rourkela, is a record of an original work done by me under the guidance of **Dr. Pitamber Mahanandia**, Assistant Professor, NIT Rourkela and this project work has not performed the basis for the award of any Degree or diploma/ associate ship/fellowship and similar project if any.

Bamadev Das

Department of Physics & Astronomy
National Institute of Technology Rourkela
Rourkela-769008, Odisha, India.

Acknowledgement

- I am honestly and heartily grateful to my parents for their caring and support throughout my life.
- I would like to give my sincere gratitude to my supervisor **Prof Pitamber Mahanandia** for his continuous support in my research work, motivated thought, patience and immense knowledge.
- I am extremely grateful to chairman **Prof D.K.Bisoyi** (H.O.D) and M.S.C members **Prof J.P.Kar** (PH), **Prof R. Mazumder** (CR), **Prof P.K.Tiwari** (EC), for their insightful comments and constructive suggestions to improve the quality of this research work.
- I would like to give special thanks to **Kadambinee Sa**, **Prakash Chandra Mahakul**, **BVGS Subramanyam & Sunirmal Saha** for their continuous encouragement and co-operation during my research.
- I would like to show my sincere thanks to **Mr. Radha Raman Nayak** (XRD), **Mr. Subabrata** (FESEM), **Mr. Subrat** (SEM) and **Mr. Soumik Roy** (TEM-S.N.Bose) for their selfless help in doing characterization.
- Thanks to all the faculty & staff of Department of Physics & Astronomy.
- I would like to thank **The Director, NIT Rourkela, Prof. S. Sarangi** for giving me opportunities and facilities to explore the research.
- At last but not the least, I never forget to remember all my friends & well-wishers for their blessings, love, inspiration, encouragement, and strong supports in every moments of my life.

Bamadev Das

Preface

Fabrication of Chemical Vapor Deposition (CVD) Setup & Preparation of Copper Oxide (CuO)-CdX (X= Se, S) Nanoparticles Decorated Core-Shell Heterostructure

This thesis describes the research carried at Department of Physics & Astronomy, National Institute of Technology Rourkela, Odisha, India under the supervision of Prof. Pitamber Mahanandia.

The goal of this project is to fabricate a low cost chemical vapor deposition (CVD) setup and synthesize hybrid nanomaterials i.e. copper oxide (CuO)-CdX (X=Se, S) nanoparticles decorated core-shell heterostructure. The synthesized hybrid nanomaterials have been fabricated into a device (photodetector) for the measurement of current-voltage characteristics in dark and under UV illumination. Furthermore, the growth model for the formation of core-shell heterostructure has also been discussed in this project.

Chapter-I narrates about the fundamentals of materials, nanomaterials and hybrid nanomaterials. In this chapter, the importance, properties, application of nanomaterials have been outlined. Moreover, the properties and morphology and corresponding application are highly dependent on the synthesis methods. Chemical vapor deposition (CVD) technique is found be one of versatile among all other preparation methods. The motivation by addressing the challenges have been discussed thoroughly.

Chapter-II describes the fabrication of a low cost CVD setup. For the fabrication of CVD setup, a three-zone horizontal furnace, reaction tube, a rotary van pump and three mass flow meters have been procured. A liquid precursor handling system and a reaction chamber which has fitted with two couplings have been designed. All these subcomponents have been assembled and integrated into a single unit CVD setup.

Chapter-III discusses about the detailed experimental procedure for the synthesis of CuO nanowires-CdX (X=Se, S) nanoparticles decorated core-shell heterostructure. For the synthesis of CuO-CdX (X= Se, S) heterostructure nanomaterials, CuO nanowires have been synthesized first by using thermal oxidation of Cu foil in air at 500^0C for 5 hours. These CuO nanowires grown on cu foils have been used for the synthesis of heterostructure by using the fabricated CVD. All these materials i.e. CuO nanowires, CuO-CdSe & CuO-CdS heterostructure have been characterized by field emission electron microscopy (FESEM) attached with energy dispersive spectroscopy (EDS), x-ray diffraction (XRD), transmission electron microscopy (TEM) attached with high resolution TEM (HRTEM) and selected area diffraction pattern (SAED), RAMAN spectroscopy & UV-Vis spectroscopy. Moreover, these materials have been fabricated intoa photodetector for the measurement of current-voltage characteristics in dark and under UV illumination.

Chapter-IV describes the detailed material characterization of CuO-CdSe heterostructure nanomaterials. The FESEM image of CuO nanowires reveals the formation CuO nanowires stretching out of the surface. The surface of CuO nanowires is very much smooth and impurity free. Formation of beaded like structures of CdSe is found to be attached intermittently on the

surface of CuO nanowires. The presence of Cd, Se elements in the materials has been confirmed by EDS. However, the formation of these bead structure is well confirmed TEM along with the formation of core-shell heterostructure. XRD, HRTEM, SAED pattern confirms the crystalline nature of the materials. Raman spectroscopy further confirms the presence of CdSe in the CVD synthesized materials. Using UV-Vis spectroscopy measurement the band gap is found to be ~2.2eV for CuO nanowires and 3.96eV for CuO-CdSe heterostructure.

Chapter-V discusses about the material characterization of CuO-CdS nanomaterials. From FESEM image, the rough surface of CuO-CdS is found by FESEM observation which is attributed to the deposition of CdS nanoparticles thoroughly on to the surface of CuO nanowires during preparation of CuO-CdS core-shell structure by CVD process. The presence of Cd, S elements in the materials has been confirmed by EDS. The formation of core-shell heterostructure has been well verified by TEM. The crystalline natures of the materials have been confirmed by XRD, HRTEM, and SAED pattern. Raman spectroscopy further confirms the presence of CdS in the CVD synthesized materials. The band gap is found to be ~3.73eV for CuO-CdS heterostructure as measured by UV-Vis spectroscopy.

Chapter-VI discusses about some general trends in growth mechanism of hybrid nanomaterials and a probable growth mechanism of the present research work has been suggested as deduced from experimental characterization. The probable growth mechanism for CuO-CdSe is found to be gas phase adsorption, whereas surface diffusion and gas phase adsorption growth mechanism for CuO-CdS has been suggested. However, the exact growth mechanism is yet to be established that needs further investigation in detail. Furthermore, the current-voltage characteristics of the fabricated photodetector have been measured by Keithley source meter 2400. The measured current for the CuO is 1.4μA at bias voltage 3 Volt. Similarly,

the dark current measured for the CuO-CdSe is 11 µA. However, the current increased to 33µA under UV illumination at the biasing 3V. For CuO-CdS, the current is found to be 10.8µA and increased to 23.8 under UV illumination at the biasing 5V. The increase in photocurrent attribute because of the effective charge separation in electron-hole in the heterojunction, which has been discussed thoroughly in the chapter by using band diagram.

CONTENTS

List of figures

Chapter-I

General Introduction to Nanomaterials

&

Scope of the Thesis

1.1 Introduction

Materials have always played a significant and defining role in human development. Materials are central to our prosperity and new materials hold the key to our future development**.** To develop the new products and technologies that will make our lives safer, more convenient, more enjoyable and more sustainable we must understand how to make best use of the materials we already have, and how to develop new materials that will meet the demands of the future. The central concept in materials science and engineering is that the properties and behaviour of every material is dependent on its microstructure, and that microstructure can be controlled by the way in which the material is made and processed. Therefore, a strong understanding of material use and manufacturing processes is essential and needed for various applications.

1.2 Nanomaterials

The reduced size of the material to the nanometer level called nanomaterial is of great interest because at this scale it shows unique and quite different, optical, electrical, thermal, mechanical and magnetic, properties compared to the respective bulk material. Nanomaterials are commonly defined as materials with an average grain size less than 100 nanometers where one nanometer is 1×10^{-9} m or one millionth of a millimeter. Nanomaterials give impetus to new applications of the nanotechnology because they exhibit novel physical properties. Nanomaterials have been considered one of the biggest discoveries of the century, which have been providing wide open and newer field for the research. Nanomaterials constitute a bridge between atomic, molecular and bulk systems. These emergent properties have the potential for great impacts in electronics, medicine, and other fields. Nanomaterials research takes a materials science based approach to nanotechnology, leveraging advances in materials metrology and

synthesis which have been developed in support of microfabrication research. Implementation and application of nanomaterials in nanotechnology depends upon the important physical properties. The important physical properties of the prepared nanomaterials depend on the production methods which control the shape, size, crystallinity etc. Moreover, application of nanomaterials depends upon precise fabrication technology [1]. Nanoscience and technology is a broad and interdisciplinary area of research. Development activity about nanoscience and technology has been growing explosively worldwide. It has the potential for revolutionizing the ways in which materials and products are created and the range and nature of functionalities that can be accessed. It is having a significant commercial impact and will assuredly increase in the future as well.

1.3 Properties and Applications of Nanomaterials

Nanomaterials show interesting optical, electrical, magnetic, thermal and mechanical properties compared to the respective bulk material. In the future, nanotechnology and the resulting nanomaterials may represent the major key for solving the most important challenges facing our society in a range of pivotal areas of fundamental needs, including energy, the environment, climate, efficient use of resources, mobility, safety, information/communication, health and food supplies [2-4]. Semiconductor nanostructured materials show narrow, tunable and symmetric emission spectra and exhibit temporal stability and resistance to photo-bleaching for which they can be used as biological levels. Semiconductor quantum dots have also been employed for in vitro imaging of pre-labeled cells. Their long-term photo-stability makes real-time and continuous monitoring possible. Moreover, semiconductors have been used in photovoltaics because of its band which can strongly absorb the solar spectrum [5-9]. Nanophase

ceramics are of particular interest because they are more ductile at elevated temperatures as compared to the coarse-grained ceramics and have got application in medical-drug delivery [10]. Magnetic nanoparticles have been studied extensively for many technological application such as magnetic storage media, bio- sensing application, medical application (such as targeted drug delivery), contrasts agents in magnetic resonance imaging (MRI) and magnetic inks for jet printing [11-23]. Metals oxide nanomaterials have also got interesting properties and probable application in nanotechnology. One of the interesting things about the metal oxides is that they can adopt a vast number of structural geometries with an electronic structure that can exhibit metallic, semiconductor or insulator characteristics [24-26]. Introduction of nanomaterials in polymer can also enhance the physical properties of respective composite that show various potential applications such as electrodes, mechanically strong, thermal tiles, EMI shielding etc. [27]. In addition to nanomaterials new classes of materials have emerged as potential hybrid nanomaterials in which heterostructure materials exist in a single unit structure.

1.4 Hybrid Nanomaterials

Hybrid materials which are the combination of two or more than two elements exist in one unit molecular structure are of great importance in science and technology due to their combined physical properties [28-33]. To make use multifunctional device application, extensive research is going on all over the world about the preparation and fabrication of hybrid nanomaterials. These types of smart materials with proper narrow size distributions and tailored physical or chemical properties have potential application in photochemical devices, ultrasensitive detection, lithium-ion batteries and heterogeneous catalysis etc [33-72].

1.5 Advantage of hybrid nanomaterials

The functional properties in hybrid nanomaterials can be readily tuned by the integration of different nanoscale building blocks (nanoparticles, nanorods, nanotubes etc.). When these nanomaterials are integrated to form new hybrid nanomaterials, the functional properties of these nanoscale building blocks may couple each other to yield newer properties. It has been observed that the hybrid nanomaterials possess novel properties different from that of isolated components or possess complementary properties. Due to its unique structure and attractive physical properties, hybrid nanomaterials have been researched for various applications such as gas sensor, chemical sensor, photovoltaics, electrochemical, photodetector, optoelectronic devices, hydrogen generation, catalytic application and many more. The hybrid nanostructured materials are also some time superior advantage as compared to nanomaterials depending upon the applications. The range of hybrid nanostructured materials covers metals, metal oxides, metal chalcogenides, polymers, carbonaceous materials, etc. Moreover, such hybrid nanomaterials with morphologies such as zero dimensional (0D) nanoparticles, 1D nanowire/ rods/ belts, 2D nanosheets/plates and 3D porous frameworks/networks [73-80] have been already reported. The applications of hybrid materials are electrochemical capacitors [81], photocatalytic activity [82], lithium-ion batteries [83], photodetector [84], solar cell [85], photoelectrochemical water splitting [86], optoelectronic conversion devices [87] etc..

1.6 Different Hybrid Nanomaterials

There are various one dimensional heterostructure synthesized such as Ag-CuO [88], Pd-CuO [89], Au-CuO [90], ZnO-CuO [91], CuO-ZnO [92], CdS-CuO [93], CdS-ZnO [94], CdSe-ZnO [95], etc. In this context, among other hybrid nanomaterials, CuO and Cu_2O are ideal materials for heterostructure because of its ideal band gaps, low cost, non-toxic and catalysts free fabrication. It has been reported that copper oxide nanomaterial the p-type semiconductor in core with a n-type shell forming core-shell heterostructure architecture may enhance the photoresponse of such material [96-107]. Furthermore, CdSe and CdS is n-type promising II-VI compound semiconductor with excellent optoelectronic properties in the visible region. A wide variety of one-dimensional CdSe & CdS nanostrcutures have been synthesized and fabricated into photodetectors with excellent performance in the visible-light region, such as large photocurrent to dark current ratio, short rise time and decay time [142-143]. It has been reported that the photocurrent to dark current ratio for these semiconductor can be enhanced by the formation of heterojunction [142]. Therefore this reflects that it would be of great interest to develop high efficient CuO-CdX(X=Se, S) core-shell heterostructure with CuO nanowire as core and CdX forming shell structure resulting a unique hybrid material with interesting properties for various applications that bears interesting to investigate. Controlled synthesis of hybrid nanostructured materials with desired shape, size and crystallinity is technologically important [108, 109]. Current status of the CuO and CdX(X=Se, S) have been reviewed and stated in brief. Following chemical bath deposition technique CuO-CdS core-shell hetero-structure nanowires have been prepared by El Mel et al. It has been extensively studied in this paper that the thickness of CdS shell is dependent on the diameter of the CuO core [110]. The enhancement of photocatalytic properties of the material by decorating Au on CuO nanowires

have been reported by Yu et al. [111]. Zhao et. al. has investigated about the Ag nanoparticles decorated CuO nanowires for efficient plasmon enhanced photoelectrochemical water splitting properties [112]. The fabrication of ZnO/CdS core/shell nanowires by solution method has been reported by Tal et. al [113] for the application in solar energy conversion. Guo et. al have reported the synthesis of ZnO/CuO hetero-hierarchical nanotrees array [114]. Here, CuO nanowires are prepared by thermal oxidation and then chemically treated for the synthesis of ZnO/CdS heterostructure [115]. The electrochemical fabrication of ZnO-CdSe core-shell nanorods arrays for the application in photoelectrochemical water splitting has been reported by Miao et. al.[116]. Landi et. al. has described about CdSe quantum dots decorated carbon nanotubes (CNTs) for solar cell application, prepared by solution method [117]. Using chemical vapor deposition technique, Yu et. al. has reported about the synthesis of CdSe nanocrystal-carbon nanotubes hybrid nanostrcutures [118]. The synthesis of CNT –CdSe by solution method for the application the photocatalytic activity of the composites, reported by Chen et. al.[119]. Beatriz H. Jua ´rez et. al. also reported about the synthesis of CNT-CdSe hybrid structure. In this paper, it has been given insights to the mechanism of CdSe attachment to the CNTs [120].

The most important thing about application of the hybrid nanomaterials are how they are prepared, because shape, size, morphology and the properties depend upon methods of preparation.

1.7 Synthesis of hybrid nanomaterials

The morphology, physical and chemical properties of the hybrid materials are highly dependent on the synthesis methods. Several strategies or synthesis methods have been reported for designing hybrid nanomaterials such as electrochemical method, hydrothermal route, chemical bath deposition (CBD), chemical vapor deposition (CVD) etc. Among all the synthesis method, chemical vapor deposition (CVD) technique is versatile technique to prepare different bulk materials, thin films, nanomaterials and hybrid nanostructure materials.

1.7.1 Chemical Vapor Deposition (CVD)

Preparation of materials in CVD involves the dissociation and/or chemical reactions of gaseous reactants in an activated (heat, light, plasma) environment. Bulk materials, thin films, nanomaterials, hybrid nanomaterials, predefined pattern growth of materials are being prepared day today by adopting CVD technique [121]. In order to prepare the above said materials CVD involves the following steps as shown in **Figure 1**.

- Mass transport of reactant gaseous species to vicinity of substrate
- Diffusion of reactant species through the boundary layer to the substrate surface or homogeneous chemical reactions to form intermediates
- Adsorption of reactant species or intermediates on substrate surface
- Surface migration, heterogeneous reaction, inclusion of coating atoms into the growing surface, and formation of by-product.
- Desorption of by-product species on the surface reaction
- Transport of by-product gaseous species away from substrate(exhaust)

Due to its process parameter, CVD has got a number of advantages in terms of preparation of nanomaterials. The advantages are being simple method, requirement of low temperature & pressure for the synthesis of nanomaterials. Furthermore, in CVD, it can be used wide variety of precursors such liquid precursors, gaseous precursors, solid precursors which include halides, hydrides, metal-organic, organic etc. It enables the usage of variety of substrate and allows materials growth in a variety of forms, such as powder, thin or thick films aligned or entangled straight or coiled nanotubes. It also offers better control on the growth process of materials. CVD allows proper control on the deposition rate, pressure temperature so as to prepare maintain the desired structure, composition and size of the materials.

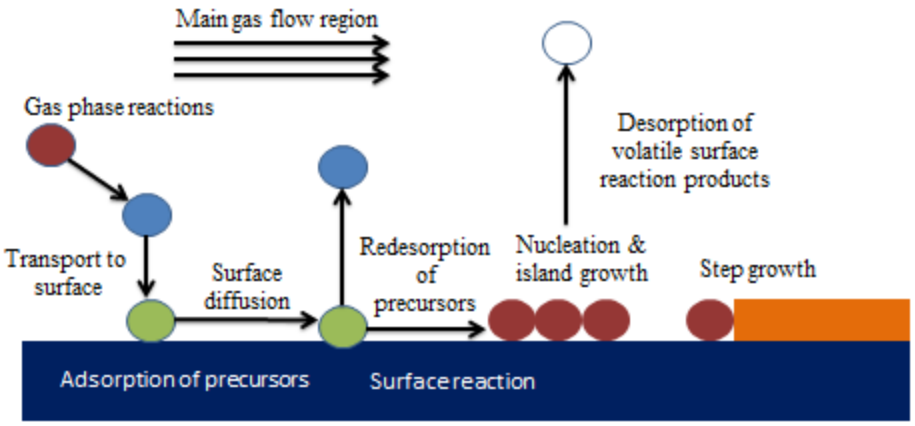

Figure 1: Shows the various steps and chemical reaction which take place during a chemical vapor deposition (CVD) deposition of materials. This reaction takes place inside the reaction chamber.

Due to its versatile nature and ability of using wide variety precursors (Source materials), CVD is a potential technique for the industrial application and laboratory research. CVD technique has been used in coating industry for making of wear resistance, corrosion resistance, layer for high temperature protection layer, erosion protection layer and many more. CVD

technique has also been used in semiconductor industry for the making of integrated circuits, sensors, optoelectronic devices, solar cell etc. As per requirement it is very difficult to fabricate dense structural part in some other preparation methods. On this regard, CVD can be used to produce components that are difficult or uneconomical to produce by using conventional fabrication techniques. Furthermore, CVD has been a technique for production of composites. Using CVD techniques, ceramic matrix composites such as carbon-carbon, carbon-silicon carbide and silicon carbide-silicon carbide composites can be synthesized. It is also used for the production of novel powders and fibres [122-141].

CVD can be modified in terms of using of energy to ignite or to activate the reaction inside the reaction chamber. High temperature CVD is predominantly used for structural material. Low temperature CVD is used where the substrate cannot sustain high temperature. In terms of process control, CVD can be modified to continuous, discontinuous and pulsed CVD (P-CVD). In terms of source of activating the chemical reaction, CVD can be modified to plasma enhanced CVD (PECVD), laser induced CVD (LCVD), photo CVD (PCVD).

The plasma-enhanced chemical-vapor deposition (PECVD) is similar to chemical-vapor deposition (CVD). The important difference is that in CVD thermal energy is used to activate the gas and in PECVD the molecules are activated by electron impact. The gas activation takes place in non-equilibrium plasma referred to as a glow discharge. The main purpose of using plasma enhancement is to reduce the activation energy for a deposition process. It has been recognized that one of the most important and unexpected benefits of PECVD growth is the alignment growth of nanomaterials due to interaction with the electric field. A PECVD system consists of a vacuum chamber, vacuum pump, a pressure control system, a gas flow control system that

includes gas in many folds, mass flow controllers and a showerhead for uniform gas mixing and distribution over the substrate; one or two power supplies for plasma excitation with corresponding power coupling systems; and a substrate heater with a temperature control system. A variety of plasma sources have been successfully used for the deposition of nanomaterials. These sources include direct-current (dc PECVD), hot-filament dc (HF-dc PECVD), magnetron type radio frequency (rf PECVD), inductively coupled plasma (ICP-PECVD), microwave (M-PECVD) and electron cyclotron resonance (ECR-PECVD). In addition, the DC, RF and microwave power are crucial for PECVD. Although many efforts have been made in improving synthesis methods, most of them follow many steps. Moreover, the complicated control and expensive or un-renewable materials are unavoidable which have limitation in reproducing the same in large scale. The additional feature in CVD like plasma or laser adds up to the value to make the CVD setup further expensive. Though the prepared materials are good in quality, the low throughput has the limitation for the large scale commercial applications. Thus, the fabrication of a low cost CVD by which materials like bulk, thin films, nanomaterials and hybrid nanomaterials with various morphology without compromising the properties is inevitable [140].

1.8 Motivation

Though the CVD is widely used technique to prepare nanomaterials, commercially available CVD equipment is quite expensive. Producing materials with low throughput using expensive CVD and low scalability of the materials has become a matter of serious concern research, application and economical point of view. Moreover, complicated control of processing parameters and many steps followed in order to obtain better quality of materials by CVD are issues to be addressed. Therefore, it is highly essential to fabricate a low cost CVD technique which can be equally competent as par the commercially available CVD for the production of nanomaterials, thin films as well as bulk materials with various morphology having desired physical properties. This has led us to fabricate a CVD setup by assembling different required accessories for the growth of materials. In this fabricated CVD technique, maximum efforts have been made to reduce the controlling parameters with easy operations. Using this fabricated CVD technique various hybrid nanomaterials have been prepared.

References

1. G. Cao, **Nanostructures & Nanomaterials: Synthesis, Properties & Applications, 2004, ISBN:1-86094-415-9**.
2. A.K. Khan, R. Rashid, G. Murtaza and A. Zahra**, J. Pharm. Res, 2014, 13(7), 1169.**
3. C.D. Guglielmo,D.R. López, J.D.Lapuente, J.M.Mallafre, M.B.Suàrez**, Embryotoxicity of cobalt ferrite and gold nanoparticles: a first in vitro approach. Reproduct Toxicol, 2010, 30, 271-276.**
4. A.K. Khan, R. Rashid, G. Murtaza and A. Zahra**, Inorgan. Chim. Acta., 2012, 393: 154-164.**
5. S.J. Rosenthal, J.C. Chang, O. Kovtun,J.R. McBride,I. D. Tomlinson, Chem. & Bio., 2011, 18 P. Alivisatos**, Nat. Biotechnol., 2004, 22, 47.**
6. J. Nanda, K.S. Narayan, B.A. Kuruvilla, G.L. Murthy, D.D. Sarma **, Appl. Phys. Lett., 1998, 72, 1335.**
7. D.S. Koktysh, N. Gaponik, J. Crewett, M. Reifer, U. Scherf, A. Eychmuller, J.M. Lupton, A.L. Rogach, J. Feldmann **, Chem. Phys. Chem., 2004, 5, 1435.**
8. V.R. Franceschi, P. Krokene, T. Krekling, E. Christiansen, **Science, 2000, 87, 314.**
9. M. Grätzel, Nature,2001,414, 338.
10. S. Sun, C. B. Murray, D. Weller, L. Folks, A. Moser**, Science, 2000, 287, 1989.**
11. M.M. Miller, G.A. Prinz, S.F. Cheng, S. Bournak**, Appl. Phys. Lett. 2002, 81, 2211.**
12. T.K. Jain, M.A. Morales, S.K. Sahoo, D.L. Leslie-Pelecky, V. Labhasetwar **, Mol. Pharm. 2005, 2, 194.**
13. I. Chourpa, L. Douziech-Eyrolles, L. Ngaboni-Okassa, J.F. Fouquenet, S. Cohen-Jonathan, M. Soucé, H. Marchais, P. Dubois**, Analyst 2005, 130, 1395.**

14. J.W. Bulte, **Mol. Med., 2006, 124, 419.**

15. M. Modo, M. Hoehn, J.W. Bulte**, Imaging 2005, 4, 143.**

16. C. Burtea, S. Laurent, A. Roch, L. Vander Elst, R.N. Muller**, J. Inorg. Biochem., 2005, 99, 5, 1135.**

17. S. Boutry, S. Laurent, L.V. Elst, R.N. Muller**, Cont. Med. Mol. Im., 2006, 1, 15.**

18. L. Babes, B. Denizot, G. Tanguy, J.J. Le Jeune, P. Jallet **, J. Colloid Interface Sci. 1999, 212,2, 474.**

19. S. Fabio, D. Catherine, C. Paolo, C. Patrick, **Curr. Pharm. Des. 2005, 11, 2091.**

20. C. Corot, P. Robert, J.M. Idée, M**.** Port**, Adv. Drug Delivery Rev. 2006, 58,14, 1471.**

21. M. Modo, J. Bulte, Mol. and Cel. MR Im**., CRC Press: Boca Raton, 2007, FL**

22. S.W. Charles, J. Popplewell**, J. Endea. Vour., 1982, 6, 153.**

23. N.N. Greenwood, A. Earnshaw**, Chemistry of the Elements, Elsevier Butterworth-Heinemann, Oxford, UK, 1997,2nd edn, ISBN-13: 978-0750633659**

24. M. Fernández-García, A. Martínez-Arias, J.C. Hanson, J.A. Rodriguez**,** ***Chem. Rev.*****, 2004***, 104* **(9), pp 4063–4104**

25. F. Hussain, H. Mehdi, O. Masami, E. G. Russell**, J. of Com. Mat.,2006, 40,17,2006.**

26. G. Ghadimkhani, N.R. de Tacconi, W. Chanmanee, C. Janaky, K. Rajeshwar **, Chem. Commun., 2013, 49, 1297–1299.**

27. Y. Zhang, J. Xu, P. Xu, Y. Zhu, X. Chen, W. Yu **, Nanotech., 2010, 21, 285501.**

28. L. Lou, K. Yu, Z. Zhang, R. Huang, J. Zhu, Y. Wang, Z. Zhu**, Nano. Res., 2012, 5, 272.**

29. Y. Luo, J. Luo, J. Jiang, W. Zhou, H. Yang, X. Qi, H. Zhang, H.J. Fan, D.Y.W. Yu, C.M. Li, T. Yu**, Energy Environ. Sci., 2012, 5, 6559.**

30. J. Jiang, Y. Li, J. Liu, X. Huang, C. Yuan, X.W. Lou**, Adv. Mater., 2012, 24, 5166.**

31. J. Li, S.K. Cushing, J. Bright, F. Meng, T.R. Senty, P. Zheng, A.D. Bristow, N. Wu**, ACS Catal., 2012, 3, 47.**

32. B. Lim, M. Jiang, P.H. Camargo, E.C. Cho, J. Tao, X. Lu, Y. Zhu, Y. Xia **, Sc., 2009, 324, 1302.**

33. Dr.R. Costi, Prof. A.E. Saunders, Prof. U. Banin, **Angew. Chem. Int. Ed., 2010, 49, 4878.**

34. P.D. Cozzoli, T. Pellegrinoa, L. Manna**, Chem. Soc. Rev., 2006, 35, 1195.**

35. S. Mann**, Nat. Mater., 2009, 8, 781.**

36. Z. Spitalsky, D. Tasis, K. Papagelis, C. Galiotis**, Prog. Polym. Sci., 2010, 35, 357.**

37. S. Lee, C. Fan, T. Wu, S.L. Anderson **, J. Am. Chem. Soc., 2004, 126,5682**

38. Y. Yin, A.P. Alivisatos**, Nature, 2005, 437, 664.**

39. K.M.K. Yu, C.M.Y. Yeung, S.C. Tsang **, J. Am. Chem. Soc. 2007, 129, 6360.**

40. Y. Liu, X. Dong, P.Chen **, Chem. Soc. Rev., 2012, 41, 2283.**

41. X. Huang, S. Li, Y. Huang, S. Wu, X. Zhou, S. Li, C. L. Gan, F. Boey, C.A. Mirkin, H. Zhang**, Adv. Mater. 2014, 26, 2185.**

42. X. Huang, S. Li, Y. Huang, S. Wu, X. Zhou, S. Li, C.L. Gan, F. Boey, C.A. Mirkin, H. Zhang**, Nat. Commun., 2011, 2, 292.**

43. C. Hu, H. Cheng, Y. Zhao, Y. Hu, Y. Liu, L. Dai, L. Qu**, Adv. Mater., 2012, 24, 5493.**

44. X. Huang, Z. Zeng, S. Bao, M. Wang, X. Qi, Z. Fan, H. Zhang **, Nat. Commun., 2013, 4, 1444.**

45. Y. Liang, Y. Li, H. Wang, J. Zhou, J. Wang, T. Regier, H. Dai **, Nat. Mater., 2011, 10, 780.**

46. Z. Yin, S. Wu, X. Zhou, X. Huang, Q. Zhang, F. Boey, H. Zhang **, Small, 2010, 6, 307.**

47. Y. Li, H. Wang, L. Xie, Y. Liang, G. Hong, H. Dai **, J. Am. Chem. Soc., 2011, 133, 7296 .**

48. Q. Xiang, J. Yu, M. Jaroniec**, J. Am. Chem. Soc. 2012, 134, 6575.**

49. J. Liu, Z. Zeng, X. Cao, G. Lu, L. Wang, Q. Fan, W. Huang, H. Zhang **, Small, 2012, 8, 3517.**

50. L. Yang, S. Wang, J. Mao, J. Deng, Q. Gao, Y. Tang, O. G. Schmidt **, Adv. Mater. 2013, 25, 1180.**

51. Y. Shi, Y. Wang, J.I. Wong, A.Y. Tan, C.L. Hsu, L.J. Li, Y.C. Lu, H.Y. Yang **, Sci. Rep. 2013, 3, 2169.**

52. T. Zhu, H. B. Wu, Y. Wang, R. Xu, X. W. Lou**, Adv. Energy Mater., 2012, 2, 1497.**

53. W. Guo, F. Zhang, C. Lin, Z.L. Wang**, Adv. Mater. 2012, 24, 4761.**

54. L. Zhang, G. Zhang, H. Bin Wu, L. Yu, X. W. Lou**, Adv. Mater., 2013, 25, 2589.**

55. X. Qi, Y. Huang, C. Xue, H. Zhang**, Adv. Mater., 2012, 24, 5374.**

56. C. Guan, Z. Zeng, X. Li, X. Cao, Y. Fan, X. Xia, G. Pan, H. Zhang, H. J. Fan **, Small, 2014, 10, 300.**

57. W. Zhou, Z. Yin, Y. Du, X. Huang, Z. Zeng, Z. Fan, H. Liu, J. Wang, H. Zhang **, Small, 2012, 9, 140 .**

58. X. Huang, Z. Zeng, H. Zhang**, Chem. Soc. Rev., 2013, 42, 1934.**

59. K.S. Novoselov, D. Jiang, F. Schedin, T. J. Booth, V. V. Khotkevich, S. V. Morozov, A.K. Geim **, Proc. Natl. Acad. Sci., USA, 2005, 102,10451.**

60. H.S.S. R. Matte, A. Gomathi, A.K. Manna, D.J. Late., R. D, S.K. Pati, C.N.R. Rao, **Angew. Chem. Int. Ed., 2010, 49, 4059.**

61. Z. Zeng, Z. Yin, X. Huang, H. Li, Q. He, G. Lu, F. Boey, H. Zhang, **Angew. Chem. Int. Ed., 2011, 50, 11093.**

62. X. Huang, S. Tang, X. Mu, Y. Dai, G. Chen, Z. Zhou, F. Ruan, Z. Yang, N. Zheng, **Nat. Nanotechnol., 2011, 6, 28.**

63. X. Cao, Y. Shi, W. Shi, X. Rui, Q. Yan, J. Kong, H. Zhang., **Small, 2013, 9, 3433.**

64. W. Zhou, X. Cao, Z. Zeng, W. Shi, Y. Zhu, Q. Yan, H. Liu, J. Wangb, H. Zhang**, Energy Environ. Sci., 2013, 6, 2216.**

65. Y. Lee, W. Zhang, K. Wei, L. Lain-Jong**, Adv. Mater., 2013, 25, 756.**

66. M.L. Anderson, C.A. Morris, R.M. Stroud, C.I. Merzbacher, D.R. Rolison **, Langmuir, 1999, 15, 674.**

67. J.L. Mohanan, I.U. Arachchige, S.L. Brock**, Sc., 2005, 307, 397.**

68. M.F. Islam, L.A. Hough, J.M. Kikkawa, A.G. Yodh**, Adv. Mater., 2007, 19, 661.**

69. M. A. Worsley, P.J. Pauzauskie, T.Y. Olson, J.Biener, J. H. Satcher, T.F. Baumann**, J.Am. Chem. Soc., 2010, 132, 14067.**

70. S.M. Jung, H.Y. Jung, M.S. Dresselhaus, Y.J. Jung, J. Kong**, Sci. Rep., 2012, 2, 849.**

71. M. Rousseas, A. P. Goldstein, W. Mickelson, M. A. Worsley, L. Woo, A. Zettl**, ACS Nano, 2013, 7, 8540.**

72. L. Qiu, J. Liu, J. Z.Chang, S.L.Y.Wu, **Nat. Commun., 2012, 3, 1241.**

73. X. Huang , C. Tan , Z. Yin, H. Zhang, **Adv. Mater., 2014, 26, 2185.**

74. Y. Tak, S. Joon Hong, J. Sung Lee, K. Yong**, J. Mater. Chem., 2009, 19, 5945.**

75. Y.H. Chang, C.T. Lin, T.Y. Chen, C.L. Hsu, M.B. Bryning, D.E. Milkie, D. Choi, Y. Jang, J.H. Lee, G. H. Jeong, D. Whang, S. W. Hwang, K.S. Cho, S.W. Kim, **Sc. Rep., 4, 6714.**

76. X. Zhao, P. Wang, Z. Yan, N. Ren**, Chem. Phy. Lett.,2014, 609, 59.**

77. E. Formo, M. S. Yavuz, E. P. Lee, L. Lane, Y. Xia**, J. Mater. Chem., 2009, 19, 3878.**

78. A. Primo , A. Corma, H. García **, Phys. Chem. Chem. Phys., 2011, 13, 886.**

79. L. Liu, R. Scholz, E. Pippel, U. Gösele**, J. Mater. Chem., 2010, 20, 5621.**

80. G. Yu, X. Xi, L.Pan, Z. Bao, Y. Cui**, Nano Energy, 2013, 2, 213.**

81. J. Li, M. Cui, Z. Guo, Z. Liu, Z. Zhu**, Mat. Lett., 2014, 130, 36.**

82. M. Srivastava, J. Singh, T. Kuila, R. K. Layek, N. H. Kime, J. H. Lee **, Nanoscale, 2015, 7, 4820.**

83. Yu K, Lu G, Chen K, Mao S, Kim H, Chen J **, Nanoscale, 2012, 4, 742.**

84. Y. Chen, L. Wei, G. Zhang, J. Jiao**, Nano. Res. Lett., 2012, 7,516.**

85. J. Miao, H. B. Yang, S. Y. Khoo, B. Liu**, Nanoscale, 2013, 5, 11118.**

86. Z. Shi, C. Liu, W. Lv, H. Shen, D. Wang, L. Chen, L. Song Li, J. Jin **, Nanoscale, 2012, 4, 4515.**

87. X. Zhao, P. Wang, Z. Yan, N. Ren, **Chem. Phy. Lett., 2014, 609, 59.**

88. X. Guo , P. Diao, D. Xu , S. Huang, Y. Yang, T. Jin, Q. Wu, M. Xiang, M. Zhang **Inter. J. of hyd. energy, 2014, 39, 7686.**

89. Y. Yu, Y. Zhao, H. Sun, M. Ahmad, **Materials Letters, 2013, 108, 41.**

90. Z. Guo, X. Chen, J. Li, J.H. Liu, X.J Huang, **Langmuir, 2011, 27, 6193.**

91. J. Kim, W. Kim, and K. Yong, **J. Phys. Chem. C, 2012, 116, 15682.**

92. A A El Mel, M Buffiere, N Bouts, E Gautron, P Y Tessier, K Henzler, P Guttmann, S Konstantinidis, C Bittencourt and R Snyders, **Nanotech., 2013, 24, 265603.**

93. Z. Yang, L. Guo, B. Zu , Y. Guo , T. Xu , X. Dou, **Adv. Optical Mater., 2014, 2, 738.**

94. T.L. Nguyen, M. Michael, P. Mulvaney, **Chem. Mater., 2014, 26, 4274.**

95. W.M. Sears, E. Fortin, J.B. Webb, **Thin Sol. Films, 1983 103 303.**

96. H. M. Wei, H. B. Gong, L. Chen, M. Zi,, B. Q. Cao, **J. Phys. Chem. C, 1983, 116 10510.**

97. A. Mittiga, E. Salza, F. Sarto, M. Tucci, R. Vasanthi, **Appl. Phys. Lett., 2006, 88 163502.**

98. R.N. Briskman, **Sol. Energy Mater. Sol. Cells, 1992, 27 361.**

99. B. K. Meyer, A. Polity1, D. Reppin, M. Becker, P. Hering, P. J. Klar1, Th. Sander, C. Reind, J. Benz, M. Eickhoff, C. Heiliger, M. Heinemann1, J. Blasing, A. Krost, S. Shokovets, C. Muller, and C. Ronning, **Phys. Status Solidi b, 2012, 249 1487.**

100. B. D. Yuhas, P. Yang, **J. Am. Chem. Soc., 2009, 131 3756.**

101. M. Izaki, T Shinagawa, K.T. Mizuno, Y. Ida, M. Inaba, A. Tasaka, **J. Phys. D: Appl. Phys., 2007, 40 3326.**

102. T.Y. Tsai, S.J. Chang, T. J. Hsueh, H.T. Hsueh, W.Y. Weng, C.L. Hsu, B.T. Dai, **Nano. Res. Lett., 2011, 6,575.**

103. K.P. Musselman, A. Wisnet, D.C. Iza, H.C. Hesse, C. Scheu, J. L. Mac Manus-Driscoll, L. Schmidt-Mende, **Adv. Energy Mater., 2010, 22 E254.**

104. C.L. Kuo, R.C. Wang, J. L. Huang, C. P. Liu, C.K. Wang, S.P. Chang, W.H. Chu, C.H. Wang, C.H. Tu, **Nanotech., 2009, 20, 365603.**

105. M. Lai, S. Mubeen, N. Chartuprayoon, A. Mulchandani, M.A. Deshusses, N.V. Myung, **Nanotech., 2010, 21, 295601.**

106. X. Zhao, P. Wang, B. Li, **Chem. Commun., 2010, 46, 6768.**

107. A. El Mel1, M. Buffiere, N. Bouts, E. Gautron, P. Y. Tessier, K. Henzler, P. Guttmann, S. Konstantinidis, C. Bittencourt, R. Snyders, **Nanotech., 2003, 24, 265603.**

108. Y. Yu, Y. Zhao, H. Sun, M. Ahmad, **Mat. Lett., 2013, 108, 41.**

109. A. A. El Mel, M. Buffiere, N. Bouts, E. Gautron, P.Y. Tessier, K. Henzler, P. Guttmann, S. Konstantinidis, C. Bittencourt, R. Snyders, **Nanotech., 2013, 24, 265603.**
110. Y. Yu, Y. Zhao, H. Sun, M. Ahmad, **Mat. Lett., 2013, 108, 41.**
111. X. Zhao, P. Wang, Z. Yan, N. Ren, **Chem. Phy. Lett., 2004, 609, 59.**
112. Y. Tak, S. J. Hong, J. S. Lee, K. Yong, **J. Mater. Chem., 2009, 19, 5945.**
113. Z, Guo, X, Chen, J. Li, J.H. Liu, X.J. Huang, **Langmuir 2011, 27, 6193.**
114. A. Kargar, Y. Jing, S.J. Kim, C. T. Riley, X. Pan, D. Wang, **ACS Nano,2013, 7, 11112.**
115. M.Y. Lu**,** Y.T. Tseng**,** C.Y. Chiu, **Nanoscale, 2013, 5, 11118.**
116. B.J. Landia, S.L. Castrob, H.J. Rufa, C.M. Evansa, S.G. Baileyc, R.P. Raffaelle, **Sol. Energy Mat. & Sol. Cells, 2005, 87, 733.**
117. K. Yu, G. Lu, K. Chen, S. Mao, H. Kim, J. Chen, **Nanoscale, 2012, 4, 742.**
118. M.L. Chen, W.C. Oh, **Nano. Res. Lett., 2011, 6, 398.**
119. B. H. Jua ´rez, M. Meyns, A. Chanaewa, Y. Cai, C. Klinke, H. Weller, **J. Am. Chem. Soc., 2008, 130, 46.**
120. K.S. Yeung, Y.W. Lam, **Thin Sol. Fil., 1983, 109, l69.**
121. K.E. Spear, **Principles and Application of Chemical Vapor deposition, Pure, Appl. Chem., 1982, 54, 1297.**
122. H.O.Pierson, **Handbook of CVD, 2n edn. Noyes, Park Ridge, NJ, 1990**
123. K.L. Choy, **CVD coating. Progress in Mat. Sc., 2003, 48, 57.**
124. J. Tavares, E.J. Swanson, S. Coulombe, **Plasma Processes and Polymers 2008, 5, 759**.
125. L. Vescan, **Introduction and genrtal discusiion, 1995, B1.0:1-B1.0:12.**
126. K. Azumi, T. Ohtsuka, N. Sato, **J. Electrochem. Soc. 1987,134, 2541.**

127. H. Kakinuma, **J. Vac. Sci. Technol. 1995, 13, 2310.**

128. S. Hasegawa, M. Sakata, T. Inokuma and Y. Kurata, **J. Appl. Phys. 85, 3844,1999.**

129. Y. Li, J. Liu, **Chem. Mater.2001,13, 1008.**

130. C. R. Bhattacharjee, A. Nath, **J. Chem. Pharm. Res., 2012, 4, 706.**

131. W. Simmler, "Silicon Compounds, Inorganic", **Ullmann's Encyclopedia of Industrial Chemistry**, **Weinheim: Wiley-VCH, 2005, doi:10.1002/14356007.a24_001.**

132. S.M. Sze, **Semiconductor devices: physics and technology. Wiley-India. 2008, p. 384. ISBN 81-265-1681 X**.

133. T. Maruyama, T. Kanagawa, **Journal of the Electrochemical Society, 1994, 141,2868.**

134. Rahtu, Antti **Atomic Layer Deposition of High Permittivity Oxides: Film Growth and In Situ Studies** (Thesis). University of Helsinki, 2002, **ISBN 952-10-0646-3**.

135. M. Costello, D. Tossell, D. Reece, C. Brierley, J. Savage, "Diamond protective coatings for optical components". **Diamond and Related Materials** 1994, **3, 8, 1137, Bibcode**:**1994DRM.....3.1137C**.

136. S. Lee, Woong; Yu, Jin "Comparative study of thermally conductive fillers in underfill for the electronic components". **Diamond and Related Materials 2005**, **14, 1647. Bibcode:2005DRM....14.1647S..**

137. D.A. Glocker, S.I. Shah, **handbook of thin process technology. IOP, 1995, ISBN 0–7503–0311–5.**

138. A. Ellison, J. Zhang, J. Peterson, A. Henry, Q. Wahab, J.P. Bergman, Y.N. Makarov , A. Vorob'ev, A. Vehanen, E. Janze´n, **Mater. Sci. and Engg. 1999, B61, 113.**

139. J.H. Comfort, R. Reif, **J. Electrochem. Soc 136, 2368.**

140. L. Vescan, **Introduction and general discussion. In: Glocker DA, Shah SI (eds) Handbook of thin film process technology. Institute of Physics, Bristol, 1995, UK. B1.0:1–B1.0:12.**

141. D. Rudolph , S. Funk , M. Döblinger , S. Morkötter , S. Hertenberger ,L. Schweickert , J. Becker , S. Matich , M. Bichler , D. Spirkoska , I. Zardo , J. J. Finley , G. Abstreiter , G. Koblmüller, ***Nano Lett.*** **2013,*13*, 1522.**

142. J. Xiang , W. Lu , Y. Hu , Y. Wu , H. Yan , C. M. Lieber **, *Nature* 2006, *441*, 489.**

143. Z. Yang , L. Guo , B. Zu, Y. Guo , T. Xu , and X. Dou, **Adv. Optical Mater. 2014, 2, 738.**

Chapter-II

Fabrication of Chemical vapor Deposition (CVD) Setup

2.1 Configuration of A Chemical vapor Deposition (CVD) Setup

A standard CVD setup in general must meet the following basic requirements [1-3].

1. To control and deliver the precursors gas, carrier gas into the reaction chamber.
2. To provide energy to active the chemical reaction inside the reaction chamber.
3. To remove the byproduct gases that is created from reaction process from the reaction chamber.
4. To precisely control the processing parameters so that the quality and quantity of deposited products with reproducibility.

These are the basic requirements for CVD which must commonly be meeting for research application in laboratories. For large scale production, some additional points must be met which are throughput, economy, safety routine maintenance.

Based on these requirements, a CVD setup usually consists of several basic components [4-5].

1. Precursors delivery systems
2. Reaction chamber or reactor
3. Energy source
4. Vacuum system
5. Exhaust gas handling system

2.1.1 Precursors Delivery Systems

In CVD the precursor is delivered into the reaction camber. Solid, liquid and gas precursors are continuously being used to prepare various materials. In order to deliver the precursor in control manner, CVD requires the precursor's delivery systems. The role of this system is to generate precursor vapor and deliver it to the CVD reactor (The generated vapour of the precursor is delivered to the CVD reactor). A typical precursor delivery system generally consists of three or four delivery lines fitted with the control meter called flow meter or mass flow controller which can control the flow rate of the precursor. The salient feature of the gas, liquid and solid precursor materials have been discussed in brief [6-11].

Gaseous Precursors Delivery:

Gas precursors are used in CVD technique to prepare materials like, thin films, bulk materials, nanomaterials and quantum dots. At room temperature it is convenient to deliver the gas precursors into the CVD reaction chamber in a controlled manner as they can be directly injected into the reaction chamber by using flow meter or mass flow controller [4].

Liquid Precursors Delivery:

For liquid precursors, there are three ways to deliver the precursors into the reaction chamber which are schematically presented below.

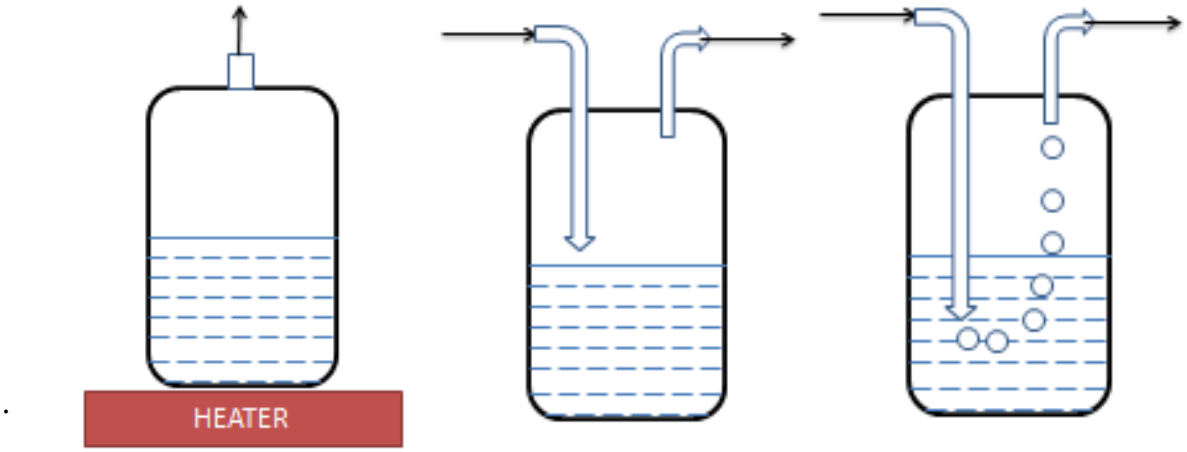

Figure 2: Schematic of delivery of liquid precursors [10] (a) direct vaporization, (b) carrier gas sweeping & (c) bubbling method

Figure 2(a) is the process in which the liquid precursor is directly heated to the vaporization point and then introduced into the chamber without using carrier gas. By using carrier gas also liquid precursor is transported to the reaction tube of the CVD as shown in **Figure 2(b)**. The last one is bubbling method (**Figure 2(c)**). In this method, the carrier gas is dipped into the liquid precursors to create continuous and homogeneous mixture of gases which can be introduced into to the reaction chamber of CVD [10].

Solid Precursors Delivery:

Unlike liquid and gas precursors, solid precursors exhibit some difficulties in introducing into the CVD reaction zone. In that case the solid precursor is heated to boiling point in order to generate precursor vapor that could be transported by carrier gas into the reaction chamber. The precursor vapor generation could be done two different ways. Firstly, the solid precursor materials having low boiling point (below 200^0C) could be preheated externally and generated vapor could be transported to the reactor with the help of carrier gas. Secondly, the solid

precursor materials having boiling points above ~200-600^{o}C could be heated in the low temperature zone of furnace in the CVD. Then the generated vapor could be introduced into the reaction zone (High Temperature Zone-2) by carrier gas [11].

2.1.2 Reaction Chamber or Reactor

A reaction chamber in the reaction tube or reactor is the heart of the CVD setup, in which the CVD reactions take place. Considering the function of the reaction chamber, it can be divided into three different zones i.e. Zone 1, Zone 2 and Zone 3. The Zone 1 and Zone 3 are usually maintained with low temperature. The most important is the Zone 2 where most of the CVD reaction takes place to form the desired material. The CVD reactor consists of the following parts [4, 5].

- A alumina or quartz tube
- Couplings to hold the pressure and keeping isolation from the rest of the environment.
- Inlet & Outlet for the flow of gas into the chamber

2.1.3 Energy Source

There are several suitable energy sources to heat CVD reaction tube which mainly include resistance heating, radiant heating, electric induction heating, laser heating, magnetic induction heating CVD, rapid thermal annealing CVD using halogen lamp heating, Joule heating CVD, and resistively heated stage CVD. Resistive heating involves the flow of current through a resistive material. Radiant heating is the heating in which heat is being transmitted via convection or conduction. Induction heating is the process of heating through electromagnetic induction in which the heat is created by the eddy currents. In laser heating, the laser is used to

heat the materials surface. For materials growth, temperature uniformity within the reactor is one of the key parameter to be precisely controlled for CVD process depending upon requirement [4, 5, 12-21].

2.1.4 Vacuum System

A vacuum system is usually used in CVD to provide continuous and uniform pressure throughout the CVD process. This helps in growing homogeneous and better quality materials. This vacuum system usually consists of pumps, valves, gauges and pipes connected together. Different types of pumps commercially available are used in CVD to maintain pressure and prepare the desired materials. Vacuum pumps can be categorized into two types depending on whether displacing or trapping the gas molecules i.e. Displacement pumps & Gas trapping pumps. Displacement pumps remove the gas molecules physically. Gas trapping pumps depend on the condensation of gas molecules within the low pressure state. Vacuum pressure pumps are also categorized according to its pressure range such as rotary van pump (10^{-2}-10^{-3} Torr), reciprocating load on clean systems (2 x 10^{-2} Torr), rotary piston pump (1-10 Torr), roots pump (10^{-4} Torr), diaphragm pump (1-10 Torr), hook & claw pump (1 Torr), screw pump (10 -3 Torr) and scroll pump (10^{-2} Torr) [4, 5].

2.1.5 Exhaust Gas Handling Systems

The role of gas handling system is to make clean, non-toxic, hazardless of reacted byproducts of CVD reaction before injecting into the open atmosphere. In order to do so, there are various processes available for safety treatments which are briefly described below [4].

(i)Cold Trap

Cold trap is a cryogenic device which is used to condense and collect the toxic gases. Since it is a cryogenic device, it uses the low temperature to condense and trap the hot toxic gases that is coming out of the reactor.

(ii)Chemical Trap

A chemical trap is generally used to protect against a corrosive which pollutes the environment and to human health. A certain types of chemical reagent are being used in this system with which the toxic gases react and trapped in the system [4].

(iii)Particle Trap

A chemical trap is generally used to protect against a corrosive which pollutes the environment and to human health. A certain types of chemical reagent are being used in this system with which the toxic gases react and trapped in the system

(iv)Wet Scrubber

This system is used to neutralize the acidic byproducts by passing the reactants through NaOH solution. Different stages like water and filter have been employed in order to make the safety efficiency higher.

(v)Venting

Venting is used to avoid the accumulation of the toxic gases under any situation which happen due to leakage of gases during a CVD process.

2.2 Fabrication of A CVD Setup

A proactive design has been made in order to fabricate CVD setup. The following parts have been procured and integrated by fabrication to make a complete CVD system as shown in **Figure 3.**

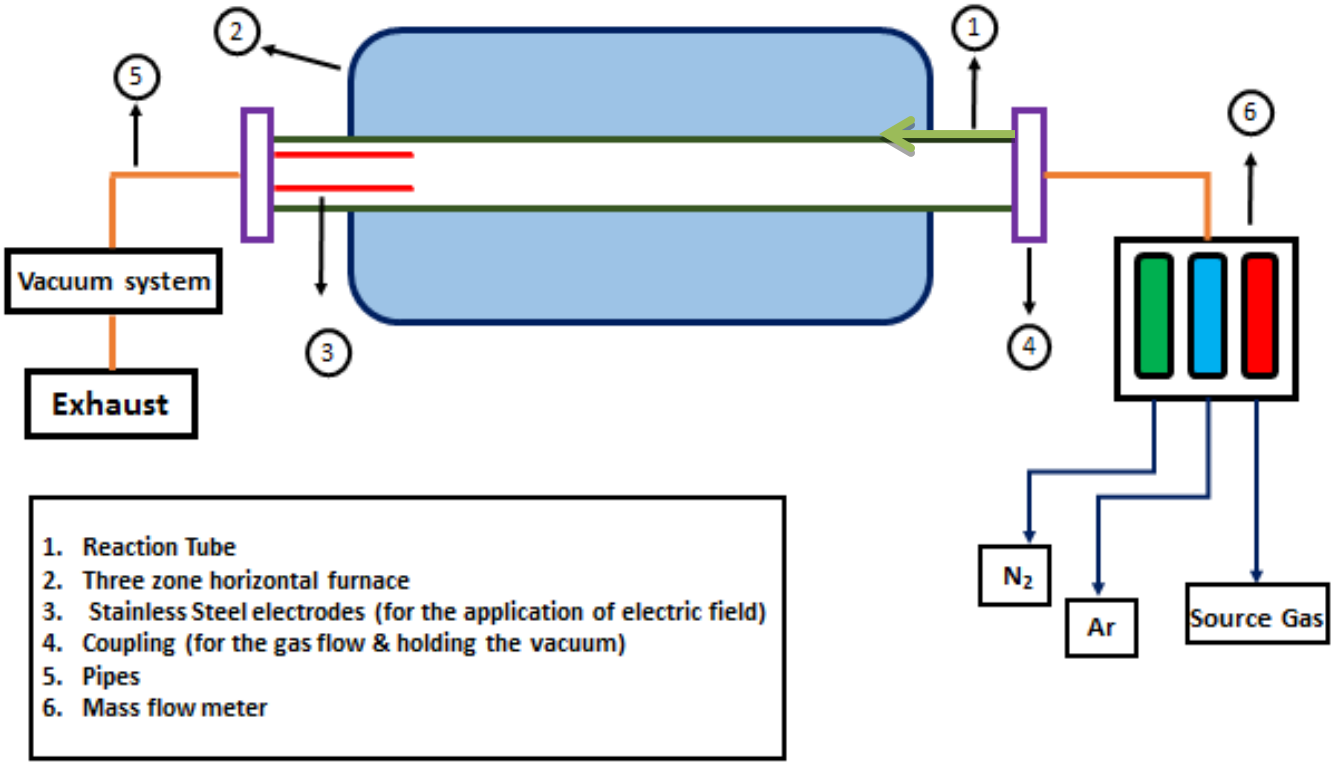

Figure 3: Schematic diagram of self-fabricated CVD setup

The schematic diagram of designed and fabricated CVD setup is shown in **Figure 3**. Three mass flow meters have been connected to the precursor delivery pipes to control and deliver precursor into the reaction chamber. These carrier gases passes through the mass flow meter and mixed at the inlet of the reaction chamber before entering into the reactor. The carrier gas has been used to carry the precursor materials into the reaction chamber in the reaction tube of CVD. The designed and fabricated complete reaction tube has been kept inside a three zone horizontal furnace. At the other end (Exit Site), a rotary van pump has been used to maintain

constant pressure throughout the CVD process, followed by an exhaust system for the collection of toxic gas that is coming out of the reaction inside the reaction chamber. In order to fabricate chemical vapor deposition (CVD) setup, following subsystems have been procured & designed with detailed specifications.

2.2.1 Procured Subsystems

- ***A three zone horizontal furnace with energy sources***

  Heating zone: 70 cm

  Heating element: Silicon carbide

  Maximum Temperature: from 100-1500^{0}C

- ***Mass flow meter***

  To control the delivery of precursors gas, carrier gas

  Maximum flow rate: 27 lpm (N_2), 22 lpm (Ar), 25 lpm (O_2)

- ***A rotary van pump for creating vacuum:***

  Maximum vacuum**:** Max pressure- 10^{-3} Torr

All the procured subsystems are shown in the **Figure 4**.

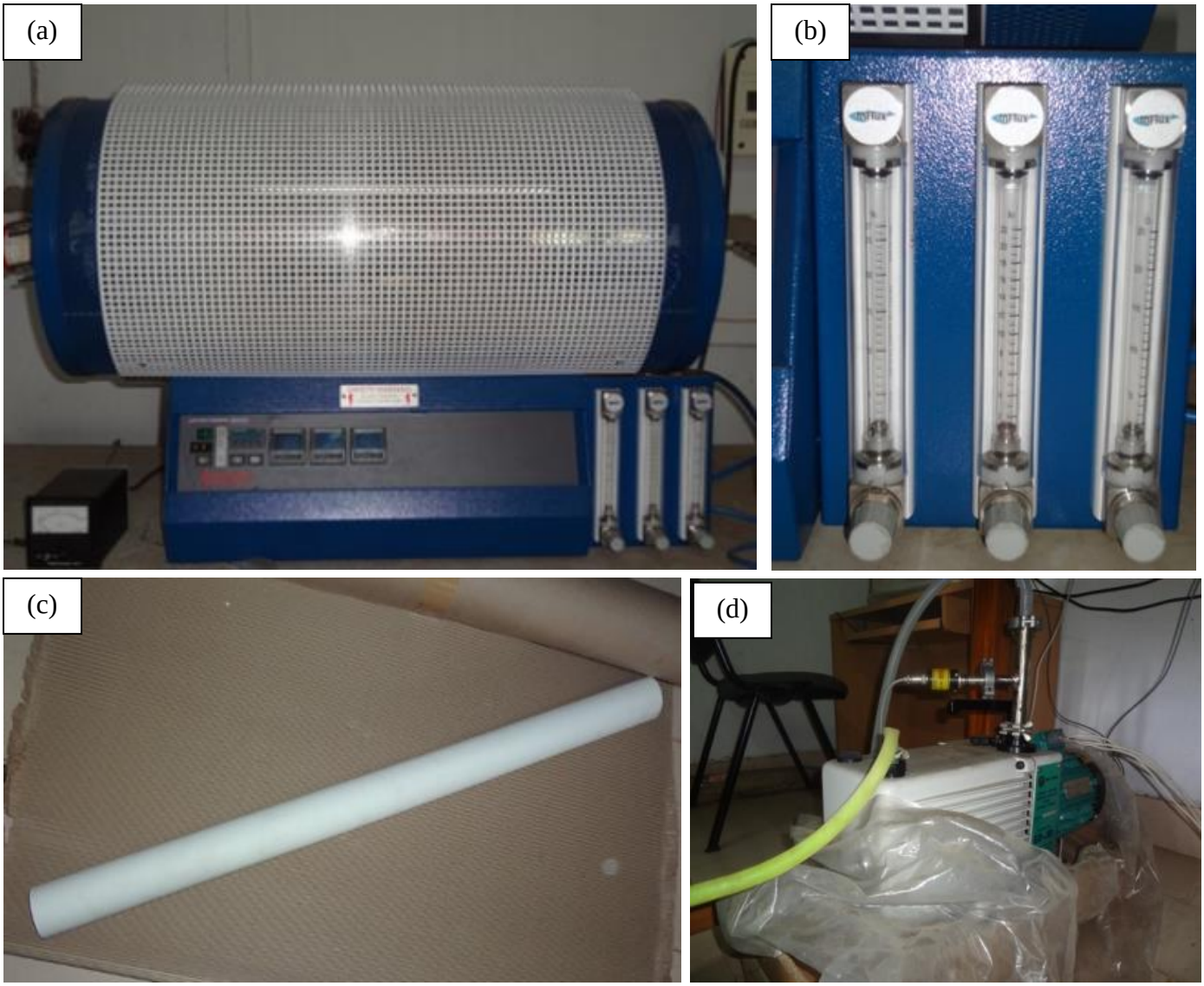

Figure 4: Digital photographs of (a) A three zone horizontal furnace; (b) mass flow meter; (c) Reaction tube (alumina); (d) Rotary van pump, respectively. All these subsystems have been procured for the fabrication of CVD setup.

2.2.2 Designed Subsystems

(i) Design of Reaction Chamber

.

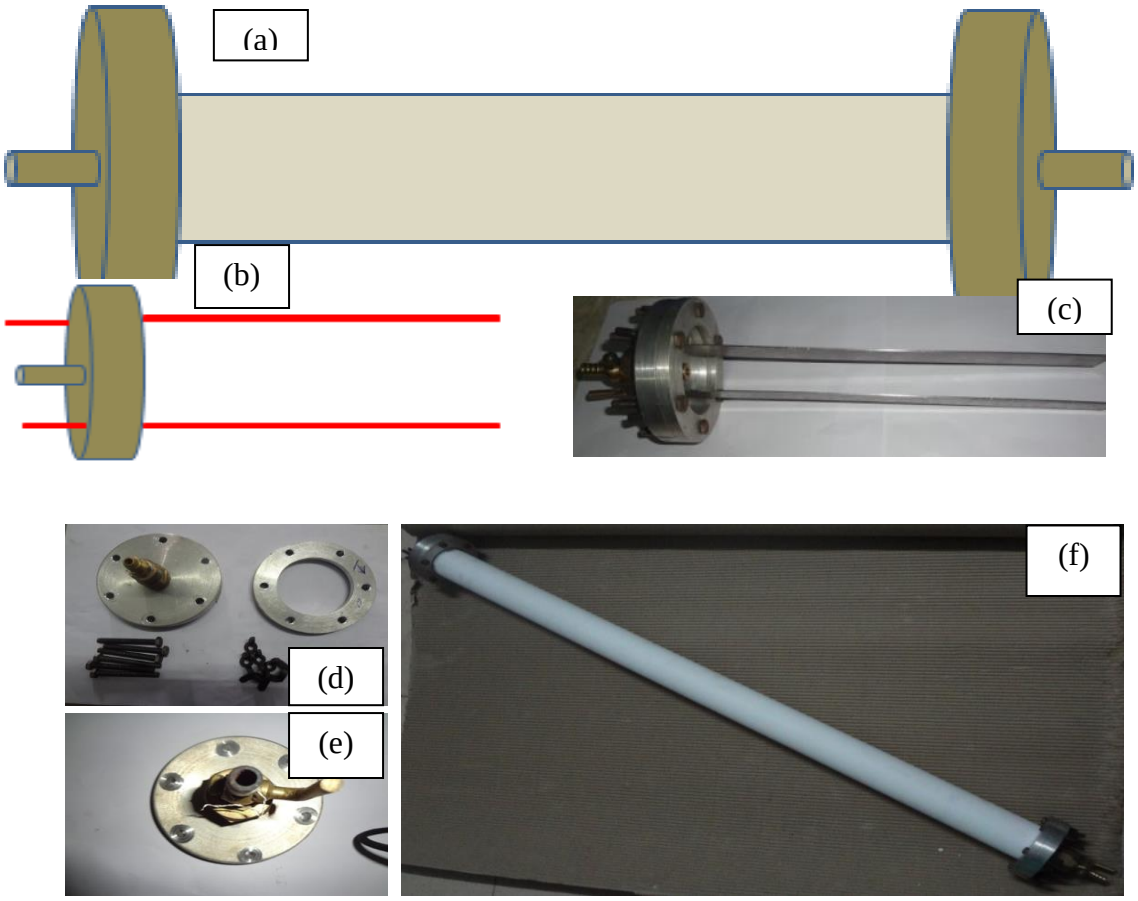

Figure 5: Animated diagram of (a) Designed Reaction Chamber; (b) Coupling for holding the vacuum and for the flow of gas in which two parallel metal electrode (red line) has been installed for the application of electric field in the reaction chamber. This will be fitted at the downstream of the tube; Digital photograph of (c) Couplings fitted with two metal electrode; (d), (e) coupling without any metal electrode; (f) the complete set of designed reaction chamber for CVD.

The detailed diagram and digital photograph of the designed CVD reactor is shown in the **Figure 5**. Two coupling having inlet and outlet are fitted to either end of the alumina tube in order to hold up the vacuum. From the inlet side the precursor materials are introduced with the help of carrier gas. A vacuum pump has been connected to the outlet of the reaction tube. Role of the vacuum pump is to evacuate the unwanted materials and maintain constant pressure during CVD process. One of the couplings is fitted with metal electrode which will be kept at the downstream of the reactor tube in order to prepare nanomaterials in the presence of electric field (**Figure 5(b), (c)**). The complete setup of reaction chamber has been shown in **Figure 5(**f).

(ii) Design of Liquid Precursors Delivery System

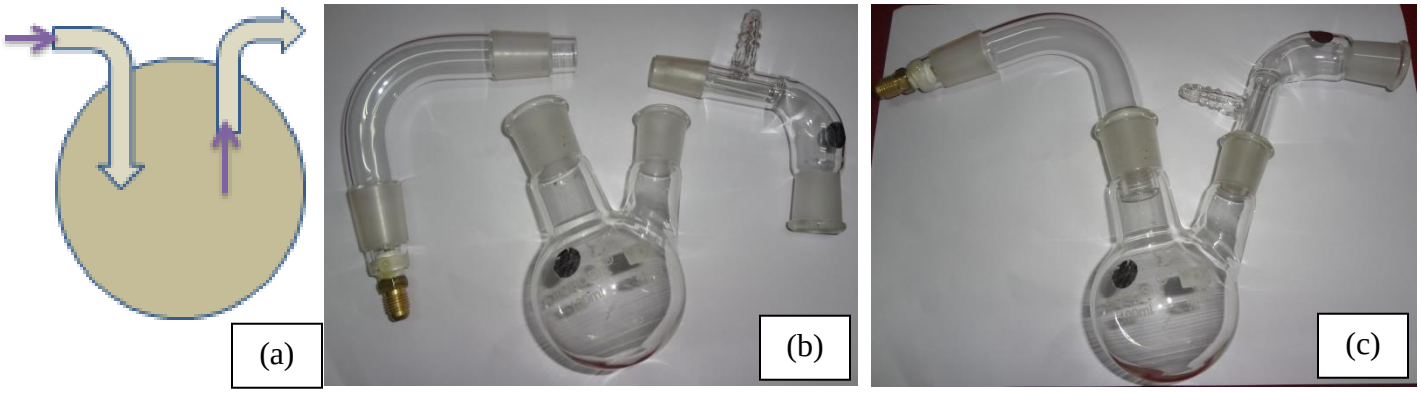

Figure 6: (a) Animated photo of liquid precursor delivery system; Digital photograph of (b) Components of liquid precursor delivery systems; (c) Designed liquid precursor delivery systems.

To prepare nanomaterials from gas and liquid precursor materials the CVD setup design has been modified. It is comparatively easy to control the flow of gas precursor for the preparation of nanomaterials by CVD. However, it is difficult to have the precise control over

the liquid precursor. Therefore, to introduce the liquid material a liquid delivery system that comprises an inlet & outlet has been fitted to a round bottom flask inside which liquid precursor is contained. The system has been fitted to reaction chamber externally and the precursor can be heated or directly injected into the chamber with help of carrier gas flow.

2.3 Fabricated CVD Setup

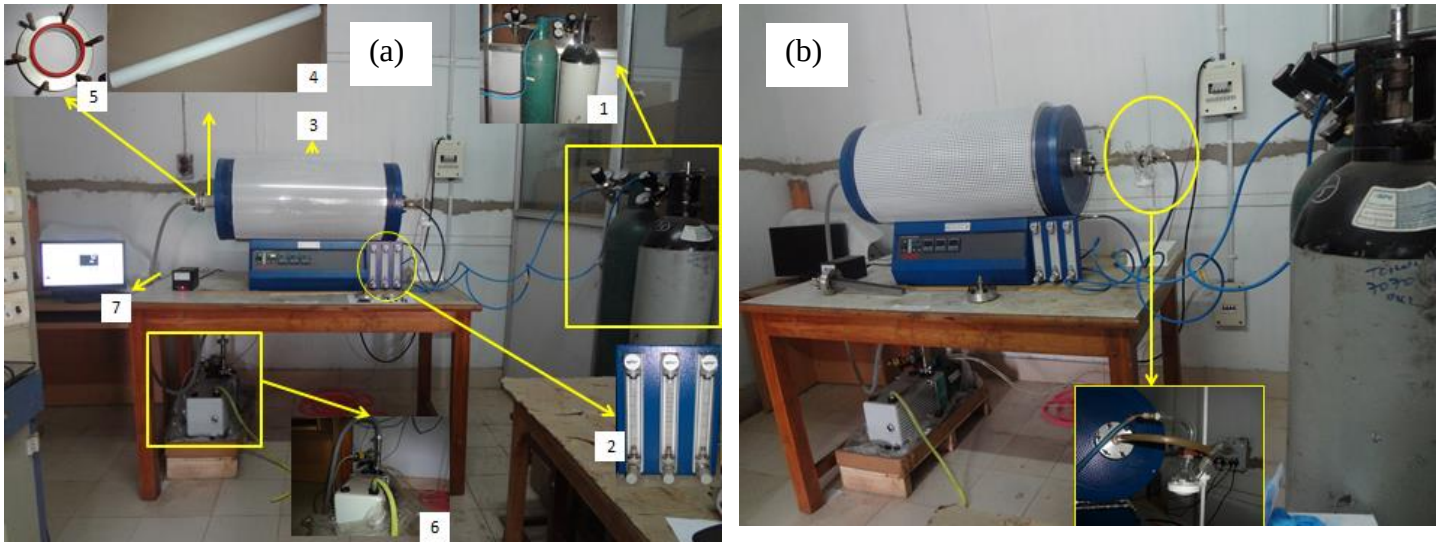

Figure 7: (a) Digital photograph of Self-fabricated CVD Setup; (b) Self-fabricated CVD Setup with an arrangement for liquid precursor delivery system (shown in yellow color dashed line).

Figure 7(a) shows the digital photograph of fabricated CVD setup in which three flow meters **(No. #2)** have been installed in order to control delivery of carrier gases and precursors gases **(No. #1)**. According to our fabricated CVD setup, the gases are flown from right to left through the reaction chamber **(No. #4)** in which chemicals, substrates have been kept. In order to ignite the chemical reaction, the reaction chamber is kept inside the furnace **(No. #3)**. From the

left end i.e. downstream region, a vacuum pump **(No. #6)** has been used in order to maintain a constant vacuum pressure throughout the CVD process. A vacuum gauge **(No. #7)** has been installed along with the pump to monitor the pressure inside the reaction chamber. Using company provided software and GPIB device the CVD setup has been interfaced with the computer in order to control the processing temperature. **Figure 7(b)** shows the CVD setup in which the liquid precursor delivery system has been installed externally for the usage of liquid precursors to make the synthesis of different materials. Rest of the process is same when a gas precursor is used to prepare materials. The liquid precursor delivery system is shown in yellow line in the figure.

2.4 Summary

- A low cost CVD setup has been fabricated successfully by assembling all the required subsystems such as a three zone electric furnace, reaction chamber, mass flow meter and a rotary van pump.
- Further improvisation has been done by the inclusion of metal electrode at the downstream of the reactor tube.
- Liquid precursor delivery system has been designed to inject liquid precursors externally.

References

1. W. Kern, V.S. Ban, **CVD of inorganic thin films. In: Vossen JL, Kern W (eds) thin film processes. Academic, 1978, New York, 257-331.**
2. M.L. Hitchman, K.F. Jensen, **CVD: principle and applications. Academic, New York, 1993.**
3. G. R. Amiri, S. Fatahian, S. Mahmoudi, **Mater. Sci. Appl., 2013, 4, 134.**
4. Y. Xu, X. Yan**, Chemical vapour deposition: An integrated engineering design for advanced materials**, **Springer, 2010, e-ISBN 978-1-84882-894-0.**
5. A.C. Jones, M.L. Hitchman, **Chemical vapour deposition: Precursors, process and applications**, **RSC publishing, 2009, ISBN 978-0-85404-465-8.**
6. J.P. Senateur, F. Weiss, O. Thomas, R. Madar, A. Abrutis, **US patent 9 308 38; EU patent, 1999, 9, 858.**
7. J.F. Roeder, T.H. Baum, S.M. Bukideau, G.T. Stauf, C. Ragaglia, M.W. Russel, P.C. Van Buskirk, **Adv. Mater. Opt. Electron., 2000, 10, 145.**
8. Y. Senzaki, A.K. Hochberg and J.A.T. Norman, **Adv. Mater. Opt. Electron., 2000, 10, 93.**
9. G. Garcia, J. Caro, J. Santiso, J.A. Pardo A. Figueras and A. Abrutis, **Chem. Vap. Deposition, 2003, 9, 279.**
10. H.J. Boer, **J Phys., 1995, IV5:C5-961-966.**
11. K. Kawahara, K. Fukase, Y. Inoue, E. Taguchi, K. Yoneda, CVD spinel on Si, in G W Cullen, **Proceedings of the 10th international conference on chemical vapor deposition, electrochemical society, 1987, NJ, 588-602.**
12. T.H. Bointon, M.D. Barnes, S. Russo and M.F. Craciun, **Adv. Mater. 2015, 27, 4200.**

13. L. Tao, J. Lee, H. Li, R.D. Piner, R.S. Ruoff, D. Akinwande, **Appl. Phys. Lett. 2013, 103, 183115.**

14. L. Huang, Q.H. Chang, G.L. Guo, Y. Liu, Y.Q. Xie, T. Wang, B. Ling, H.F. Yang, **Carbon 2012, 50, 551.**

15. J. Ryu, Y. Kim, D. Won, N. Kim J. S. Park, E. K. Lee, D. Cho, S. J. Kim, G. H. Ryu, H.-A.-S. Shin, Z. Lee, B. H. Hong, S. Cho, **ACS Nano 2014, 8, 950.**

16. J.M. Lee, H.Y. Jeong, W. Park, **Electron. Mater. 2010, 39, 2190.**

17. K. Xu, C. Xu, J. Deng, Y. Zhu, W. Guo, M. Mao, L. Zheng, J. Sun, **App. Phys. Lett. 2013, 102, 162102.**

18. W. Cai, R.D. Piner, Y. Zhu, X. Li, Z. Tan, H.C. Floresca, C. Yang, L. Lu, M.J. Kim, R.S. Ruoff, **Nano Res. 2009, 2, 851.**

19. Y.Z Jiang, **Industrial electric furnaces, Tsinghua university press, 1993.**

20. V. Paschkis, J. Persson, **Industrial electric furnaces and appliances, Interscience, 1960.**

21. Clinton, P.A. Radnor, **Thermocouples. In: Liptak BG (ed) Temperature measurement, 1993.**

Chapter-III

Experimental Procedure for the Synthesis of Copper Oxide (CuO)-CdX(X= Se, S) Nanoparticles Decorated Core-Shell Heterostructure

3.1 Introduction

The future of nanotechnology depends on efficient methods of materials preparation. A successful technology must be transferred from its developer to its users, and in order for the nanotechnology to be more viable for the future generations, preparation of nanomaterials possessing unique physical properties is very essential. On this regard there have been various approaches for the preparation of better quality nanomaterials.

Though each and every preparation method has its own advantages and disadvantages, there is continuous effort to overcome the challenges to prepare nanomaterials with better quality so that the produced materials could be used for nanotechnology. Over the time period various techniques have evolved in order to prepare different nanostructured materials. Copper based oxide nanomaterials have also been prepared by adopting various preparation techniques. In this context, the objective material CuO have been prepared by thermal oxidation. CVD technique has been employed to prepare hybrid CuO-CdX (X=Se, S) using already grown CuO nanowires.

3.2 Synthesis of copper oxide (CuO) nanowires

Synthesis techniques of copper oxide (CuO) nanowires such as pure solution based methods, electrochemical methods, hydrothermal methods, direct plasma oxidation, thermal oxidation method [1-16] have been well reported. However, the thermal oxidation of bulk copper specimens such as copper foil, copper connecting wire, transmission electron microscopy (TEM) copper grids has been proved to be an efficient method among others because of high quality CuO nanowires growth, low cost, catalyst free and simple method [14-16, 17-19]. Furthermore, the thermal oxidation method provides highly aligned CuO nanowires with high density grown all over the surface just by heating copper bulk materials without catalyst, making it cost-

effective and large production method [20]. Hence the thermal oxidation method has been used for the synthesis of CuO nanowires.

3.2.1 Synthesis of CuO nanowires

Copper foils (0.1 mm thickness, 99.9%, Aldrich) have been used for the synthesis of CuO nanowires. These copper foils have been cleaned in an aqueous solution of 1.0 M hydrochloric acid (HCl) for 20-30 seconds. After that the Cu foils have been rinsed with deionized water in order to remove residuals oxygen contents and dust particles on the surface of Cu foils. Then the Cu foils is kept inside a horizontal tubular furnace with both ends open in order to provide continuously air which contains oxygen to substrate that helps in growing CuO. The experimental conditions for the thermal oxidation of copper foils have been chosen judiciously according to the literatures for the growth of high quality CuO nanowires [16]. The preparation temperature for the thermal oxidation is 500^0C for 4 hour with a heating rate 10^0C per minute. Then the power is switched off so that the furnace cools down to the room temperature automatically. A black, fragile product on the surface of copper foils has been recovered from the furnace to characterize the produced material.

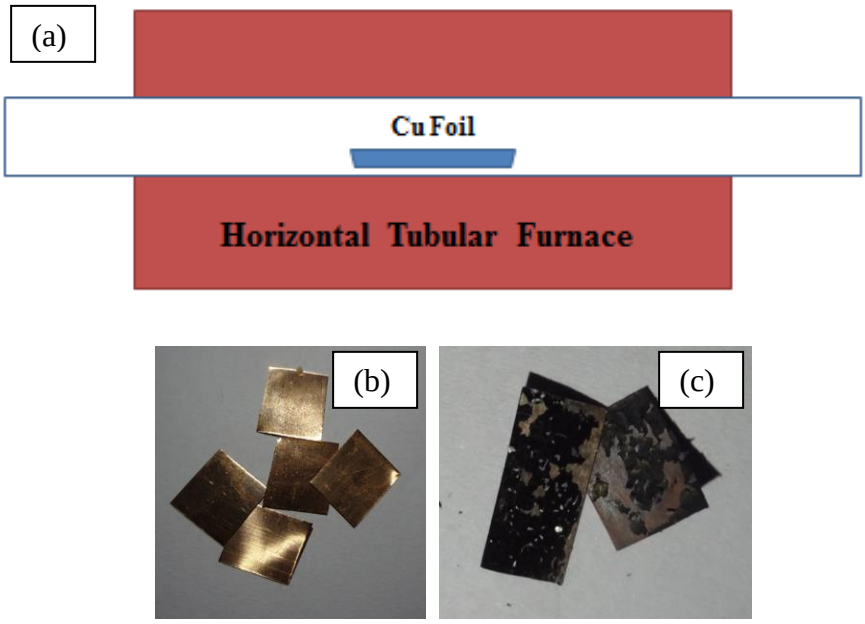

Figure 8: **(a) Schematic diagram for the synthesis of CuO nanowires using thermal oxidation, (b) Copper foils before oxidation, (c) Cooper foils after oxidation. The black materials are CuO nanowires.**

3.3 Synthesis of CuO-CdX (X=Se, S) Nanoparticles Decorated Core-Shell Heterostructure

The synthesis of CdX (X=Se, S) decorated CuO nanowires has been done by chemical vapor deposition (CVD) technique. A schematic diagram of the experimental set up is shown in **Figure 9**. The CdSe/CdS metal source is contained in a ceramic boat and kept at the middle of the horizontal tubular furnace **(Position A)** as shown in the **Figure 9**.

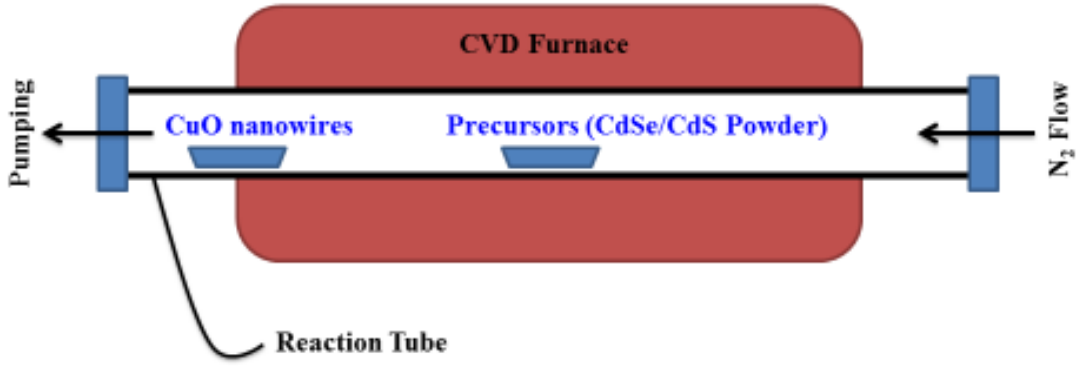

Figure 9: Schematic diagram of CVD setup for the synthesis of CuO nanowires CdX(X=Se, S) nanoparticles decorated core-shell heterostructure.

The CuO nanowires grown on Cu foils by thermal oxidation have been used as the substrate for decorating/coating CdSe/CdS particles, located at the downstream of the furnace **(Position B)**. A flow of nitrogen gas (99.999%, 1 lpm) has been used as the carrier gas, purging from one end in order to carry the CdSe/CdS vapours. A constant vacuum has been maintained (0.1 mbar) by using a rotary van pump from the other end for a constant gas flow in the reaction chamber. The reaction temperature and duration of the CVD process has been set to 400^0C for 30 minute with a heating rate of 10^0C per minute for CdSe and 500^0C for 30 minute with a heating rate of 10^0C per minute for CdS. After reaction process to the set temperature for the given time the power supply to the CVD is switched off. The furnace is allowed to cool down to room temperature. The CdSe or CdS coated material on CuO is recovered for various characterizations.

3.4 Characterization Techniques

3.4.1 Field Emission Scanning Electron Microscope (FESEM) & Energy dispersive spectroscopy (EDS)

Unlike optical microscope, electron microscope uses electrons to scan and to produce the image. Basically, scanning electron microscope (SEM) is used to study the morphology, structure of the materials at a higher resolution and magnification as compared to optical microscope.

The basic principle of SEM is that a beam of electrons is bombarded onto the surface of the materials. The bombarded electrons interact with the atoms of the sample giving rise to various signals such as secondary electrons (SE), back-scattered electrons (BSE), characteristics x-rays. The secondary electron imaging (SEI) gives the high magnified images of a sample surface. Back scattered electrons (BSE) are the electrons that have been reflected back from the sample by elastic scattering. This signal is also used for imaging but it is highly related to atomic number of the elements that are present in the sample which creates the color contrast in the image and thus help detecting different elements.

The x-rays produced by the sample are used for the elemental analysis of the material. The basic principle of EDS is that each element has a unique spectrum of x-ray which is being used to analyze the composition in the sample.

3.4.2 XRD

X-ray diffraction is a non-destructive tool which is used to identify the crystal structure, phase, crystallite size of the samples. The basic principle of the XRD is the Bragg's law i.e. **$2d\sin\theta = n\lambda$,** where λ= wavelength of x-ray, d= interlayer spacing crystals, θ= Angle of incidence, n= order of reflection.

Since the crystals are the periodic arrangement of atoms, x-rays get diffracted from the lattice points as their wavelengths are comparable to the interlayer spacing. When the Bragg's condition is satisfied in the process, XRD peak is observed in the pattern. These patterns give the information about structure, unit cell and many other parameters of the samples.

3.4.3 TEM, HRTEM & SAED Pattern

TEM is a technique in which a beam of electrons is transmitted through and interacts with an ultra-thin specimen hence forming an image which is magnified and focused onto an imaging device, such as a fluorescent screen, on a layer of photographic film, or to be detected by a sensor such as a CCD camera. The scattering processes experienced by electrons during their passage through the specimen determine the kind of information obtained. Elastic scattering involves no energy loss and gives rise to diffraction patterns. Inelastic interactions between primary electrons and sample electrons at heterogeneities cause complex absorption and scattering effects, leading to a spatial variation in the intensity of the transmitted electrons.

High-resolution transmission electron microscopy (HRTEM) is a powerful tool to study properties of materials on the atomic scale and is an imaging mode of the transmission electron microscope (TEM) that allows for direct imaging of the atomic structure of the sample. The highest point resolution realized in phase contrast TEM is around 0.5 angstroms (0.050 nm). At these small scales, individual atoms of a crystal and its defects can be resolved.

Selected Area Electron Diffraction (SAED) is a TEM technique to obtain diffraction patterns that result from the electron beam scattered by the sample lattice. From an SAED pattern, information about structural information of the sample like, crystalline symmetry, unit cell parameter and space group etc. can be obtained.

3.4.4 RAMAN Spectroscopy

Raman spectroscopy provides information about molecular vibrational, rotational and other low frequency modes of systems that can be used for sample identification and quantitation. It provides an analytical tool for molecular finger printing as well as monitoring changes in molecular bond structure.

This technique involves shining a monochromatic light source on a sample and detecting the scattered light, a very small amount of which is shifted in energy from the incident frequency due to interactions between the incident electromagnetic waves and the vibrational energy levels of the molecules in the sample. Plotting the intensity of this "shifted" light versus frequency results in a Raman spectrum of the sample.

3.4.5 UV-Vis Spectroscopy

Ultraviolet-visible spectroscopy (UV-Vis or UV/Vis) refers to absorption spectroscopy in the ultraviolet-visible spectral region.

In order to find the band gap, the equation used is,

$$(\alpha h\upsilon)^{1/n} = (E_g - h\upsilon)$$

Where α = Co-efficient of absorbance, h= Plank's constant, υ = Frequency of UV,

E_g= Bandgap of the material, n= ½ for direct allowed transition.

3.5 Summary

- The CuO nanowires have been synthesized by thermal oxidation method of Cu foil at 500^0C for 4 hour.
- These CuO nanowires grown on Cu foil have been used as substrate in CVD for the synthesis of CuO-CdX (X=Se, S) decorated CuO nanowires core-shell heterostructure.
- The temperature and time of CVD process is 400^0C for 30 minutes for the synthesis of CuO-CdSe core-shell heterostructure and 500^0C for 30 minutes for the synthesis of CuO-CdS core-shell heterostructure.
- The prepared samples i.e. CuO nanowires, CuO-CdSe core-shell heterostructure and CuO-CdS core-shell heterostructure have been characterized by FESEM, EDS, XRD, TEM, HRTEM, SAED pattern, Raman spectroscopy and UV-Vis spectroscopy which are discussed in Chapter-IV and Chapter-V.

References

1. G Filipič and U Cvelbar, **Nanotech., 2012, 23, 194001.**
2. W.Z. Wang, G.H. Wang, X.S. Wang, Y.J. Zhan, Y.K. Liu and C.L. Zheng, **Adv. Mat. 2002, 14, 67.**
3. Y. Li, Xiao-Yu Yang, J. Rooke, G. V. Tendeloo, Bao-Lian Su, **J. colloid Interface Sci. ,2010, 348, 303.**
4. X. C. Song, Y. Zhao, and Y. F. Zheng**, Crystal Growth Des., 2007, 7, 159.**
5. C. Li, Y. Yin, H. Hou, N. Fan, F. Yuan, Y. Shi, Q. Meng **, Solid state comm., 2010, 150, 585.**
6. H. S. Shin, J. Y. Song, J. Yu, **Mat. Lett., 2009, 63, 397.**
7. Anne-Lise Daltin, A. Addad, Jean-Paul Chopart, **J. crystal Growth, 2005, 282, 414.**
8. H. Guan, C. Shao, B. Chen, j. gong, x. Yang, **Chem. Comm., 2003, 6, 1409.**
9. Y. Liu, Y. Chu, Y. Zhuo, M. Li, L. Li, L. Dong, **Crystal growth des. 2007, 7, 467.**
10. Y. Xiong, Z. Li, R. Zhang, Y. Xie, J. Yang, C. Wu, **J. Phys. Chem. B, 107, 3697, 203.**
11. M. Čerček, G. Fiipič, T. Gyergyek and J. Kovačič, **Contrib. Plasma Phys, 2010, 50, 909.**
12. T.Gyergyek, B.Jurčič-Zlobec, M. Cercek, **Phys. Plasmas., 2008, 15, 063501.**
13. X. Jiang, T. Herricks, Y. Xia, **Nano Lett., 2002, 2, 12.**
14. C.H. Xu, C.H. Woo, S.Q. Shi**, Chem, Phys. Lett., 2004, 399, 62.**
15. L.S. Huang, S.G. Yang, T. Li, B.X. Gu, Y.W. Du, Y.N. Lu, S.Z. Shi, **J. Cryst. Growth, 2004, 260, 130.**
16. G Filipič and U Cvelbar**, Nanotechnology , 2012,23, 194001.**
17. B. J. Hansen, G. Lu, and J. Chen, **J. Nanomater. 2008, 830474, 2008.**

18. L. Yuan, Y. Wang, R. Mema, G. Zhou, **Acta Mater. 2011, 59, 2491**

19. A A El Mel1, M Buffiere, N Bouts, E Gautron, P Y Tessier,K Henzler, P Guttmann, S Konstantinidis, C Bittencourt, R Snyders **, Nanotechnology, 2013, 24, 265603.**

20. X. Zhao, P. Wang, Z. Yan, N. Ren**, Chem Phys Lett, 2014, 609, 59.**

Chapter-IV

Characterization of Copper Oxide (CuO)-CdSe Nanoparticles Decorated Core-Shell Heterostructure

4.1 Introduction

Research on applications of materials and nanomaterials has been rapidly growing. It is strongly believed that the fundamental characterization tools have the potential about scientific and technological impact, since the structural, morphological, optical properties of the nanomaterials have the greatest impact on the application of the materials. Thus, fundamental characterization tools involving nanomaterials drives the scientific understanding and makes it easy for researchers for the development of new technology.

On this note, the heterostructure prepared by our fabricated CVD i.e. CuO nanowires, CuO-CdSe core-shell have been characterized by field emission scanning electron microscope (FESEM) for morphology and nanostructure investigations, energy dispersive spectroscopy (EDS) for compositional or elemental analysis, x-ray diffraction (XRD) for phase confirmation, Raman for structural properties and UV-Vis spectroscopy for optical properties, whose fundamental principles have been discussed in Chapter-III.

4.2 Field Emission Scanning Electron Microscopy (FESEM) & Energy Dispersive Spectroscopy (EDS)

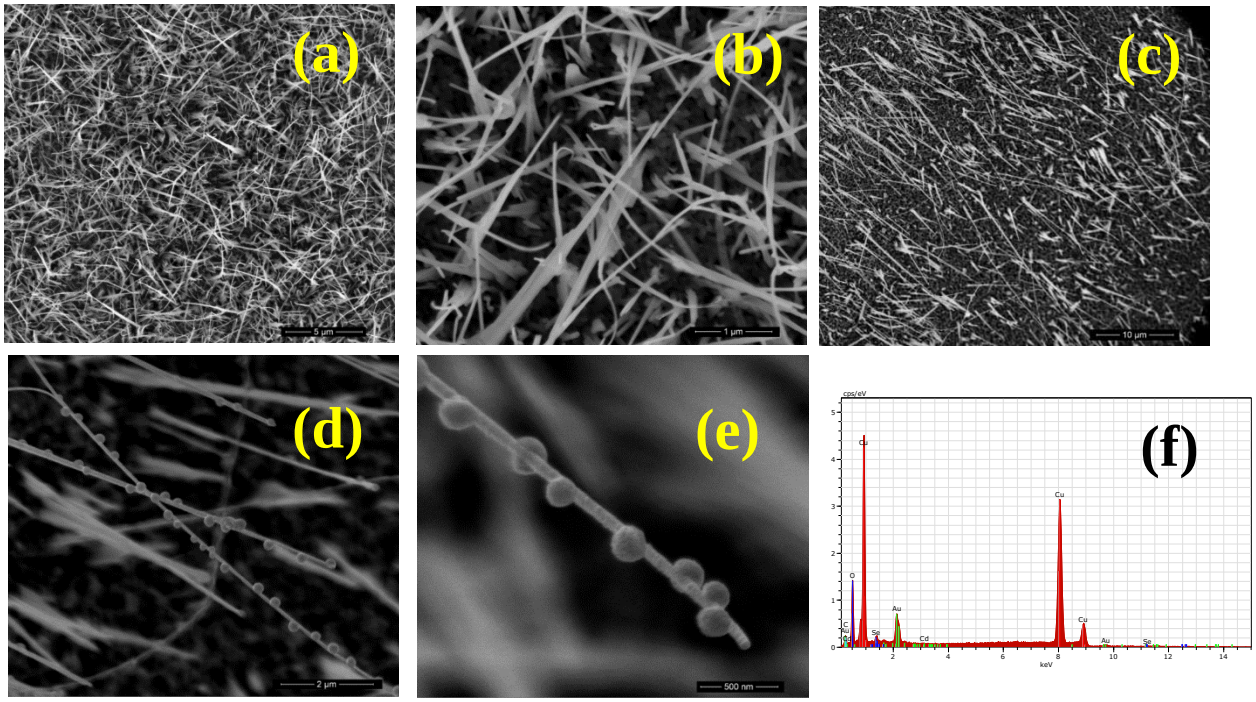

Figure 10: **(a) FESEM micrographs of CuO nanowires grown on Cu foil by thermal oxidation. (b) Magnified image of CuO nanowires, (c) Low-magnified image of CuO-CdSe nanoparticles decorated core-shell heterostructure synthesized by CVD technique, (d), (e) Magnified & High-magnified image of CuO-CdSe nanoparticles decorated core-shell heterostructure (f) EDS spectra for CuO-CdSe nanoparticles decorated core-shell Heterostructure.**

The FESEM image of CuO nanowire synthesized by thermal oxidation on Cu foil is shown in **Figure 10 (a)**. Formation of CuO nanowires on Cu foil is confirmed as observed by FESEM **(Figure 10(a)).** Thorough investigation by FESEM reveals well aligned growth of CuO nanowires throughout the surface on the Cu foil. However, there are some nanoneedles (i.e. the thickness of the nanowires decreases as we go across the length from bottom to the top) also seen in the micrographs. The lengths of the grown CuO nanowires are in the range of 1- 15 micron with average thickness approximately 0.084μm. The surfaces of the CuO nanowires along its length are smooth and no impurity particles are seen in the surface of CuO nanowires as observed in magnified FESEM image **(Figure 10 (b))**.

The low magnified FESEM micrograph CuO-CdSe core-shell heterostructure nanowire is shown in **Figure 10(c)**. For better visualization high magnified FESEM characterization has been carried out **(Figure 10(d)).** Beaded like CdSe structure onto the surface of the CuO–CdSe nanoparticles decorated core-shell heterostructure has been observed in the further high magnified FESEM **(Figure 10(e)).** After the deposition of CdSe on CuO which forms CuO-CdSe nanoparticles decorated core-shell heterostructure, the thickness of the nanowires is changed and found to be ~0.14μm. In order to check the reproducibility, the experiment has been repeated several times keeping the preparation condition fixed.

Figure 10(f) shows the EDS spectra of the CuO-CdSe nanoparticles decorated core-shell heterostructure. The EDS spectra confirm the presence of Cd, Se in the CuO-CdSe nanoparticles decorated core-shell heterostructure. The element Cu, O provides the information regarding the existence of CuO nanowires in the materials. The spectra related Au appears in the EDS spectra because of Au particles that have been deposited to the materials prior to put for FESEM characterization.

4.3 X-ray Diffraction

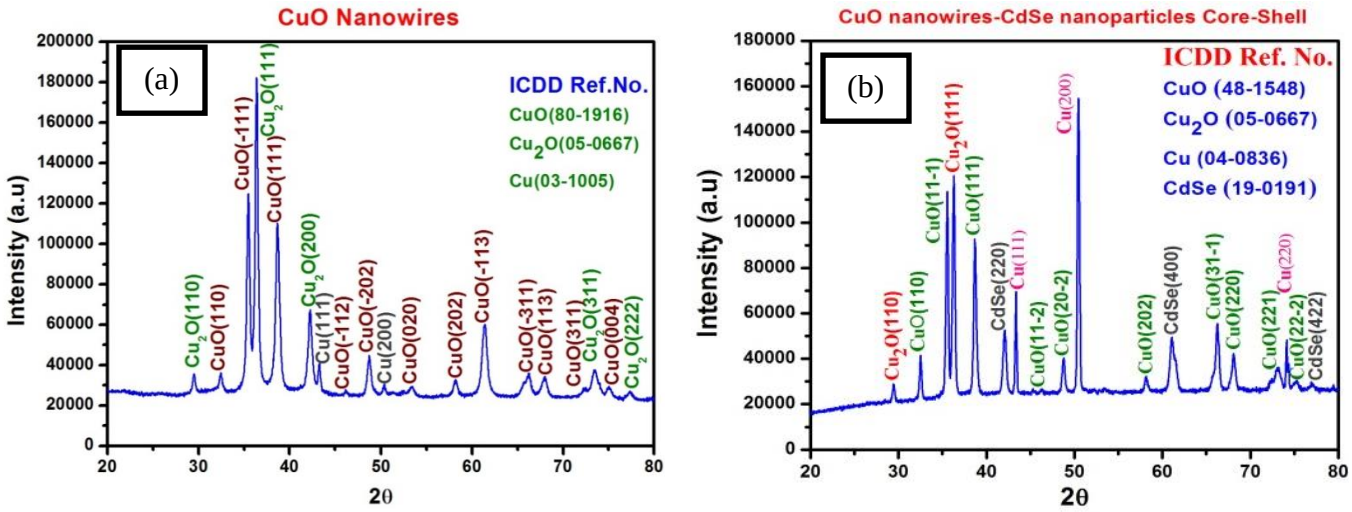

Figure 11: (a) X-ray diffraction (XRD) pattern of CuO nanowires that has been grown by thermal oxidation of bulk Cu foil, (b) X-ray diffraction (XRD) pattern of CuO-CdSe nanoparticles decorated core-shell heterostructure by using CVD technique.

The structural characterization of the CuO nanowires synthesized by thermal oxidation on copper foil has been done by XRD. Using ICDD No. – 80-1916 (CuO), 05-0667 (Cu_2O), 03-1005 (Cu) the XRD pattern of CuO has been matched. It is observed that the XRD pattern of CuO nanowires confirms the presence of CuO phase in the materials **(Figure 11(a))**. The highest intensity peak belongs to Cu_2O (111) phase. This suggests XRD pattern consists of mixed phase of Cu_2O and CuO phase. The Cu peak in the XRD pattern is due to the Cu foil which has been taken as substrate for growing CuO nanowires. **Figure 11(b)** shows the XRD pattern of CuO-CdSe core-shell nanowires heterostructure. The XRD pattern consists of CdSe phase (220, 400 and 422) along with CuO, Cu_2O, Cu phase, which confirms the presence CdSe nanocrystals in

the materials. In the XRD pattern apart from Cu, CuO and CdSe phase no other impurity peak has been observed.

4.4 Transmission Electron Microscopy (TEM)

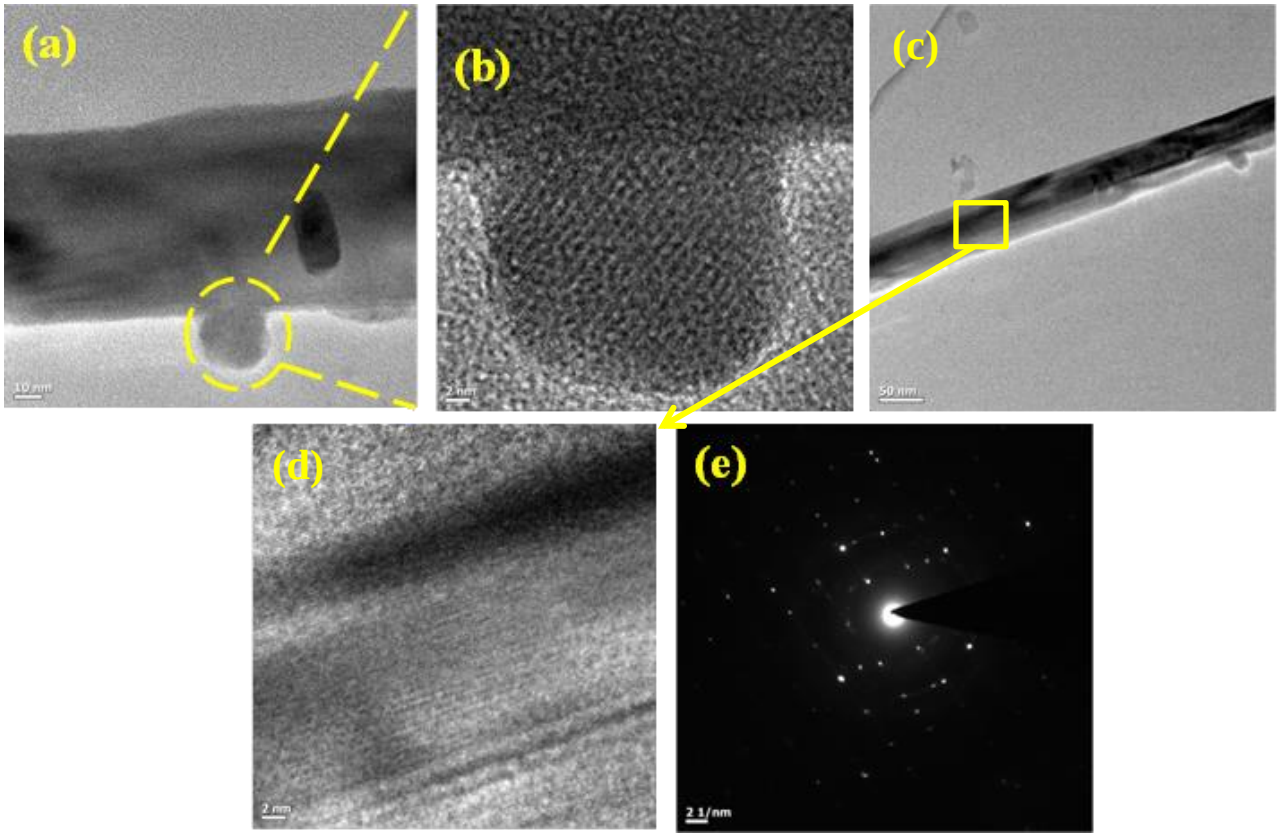

Figure 12: **(a) TEM image of CuO-CdSe nanoparticles decorated core-shell heterostructure, (b) HRTEM of CuO-CdSe nanoparticles decorated core-shell heterostructure, (C) TEM image of CuO-CdSe nanoparticles decorated core-shell heterostructure, which shows the formation of, (d) HRTEM image of CuO-CdSe core-shell heterostructure, (e) SAED pattern of CuO-CdSe nanoparticles decorated core-shell heterostructure.**

The morphology and structure of the CuO-CdSe nanoparticles decorated core-shell heterostructure a have been further analyzed by transmission electron microscopy (TEM) and high resolution TEM (HRTEM) equipped with selected area electron diffraction (SAED) at an accelerating voltage of 200 kV. For TEM characterization of the prepared CuO-CdSe heterostructure material, sample preparation for the copper grid has been done by the following way. A flake of grown CuO-CdSe/CdS material is taken from the Cu foil. The flake is immersed in ethanol and sonicated for about 20 minutes for better dispersion. Then the copper grid is dipped into the solution and taken out. The prepared coper grid is dried under the table lamp to get rid off the ethanol. Finally, the CuO-CdSe contained copper grid is placed in the sample holder of the TEM for characterization. **Figure 12(a)** is a typical TEM image of CuO-CdSe core-shell heterostructure. From TEM image it is observed that the CdSe bead particles are adhered on the surface of CuO-CdSe heterostructure. However, as observed in FESEM characterization **(Figure 10(d), (e))**, except one or two, rests of the beads coated on CuO-CdSe have gone off the structure. This might be due to the sonication where the loosely held particles and beads are detached during sonication. **Figure 12(b)** is the HRTEM image of the bead structure shown in the dashed line. The fringe pattern of the HRTEM image reveals about crystal nature of CdSe. The formation of core-shell heterostructure deposition of CdSe nanocrystal onto the surface of CuO nanowires is confirmed by observing the TEM image **Figure 12(c).** The HRTEM image **(Figure 12(d))** taken for **Figure 12(c)** confirms the crystalline nature of the core and shell materials. The observed SAED pattern **(Figure 12(f))** by TEM also confirms the crystalline nature of the synthesized materials.

4.5 Raman Spectroscopy & UV-Vis Spectroscopy

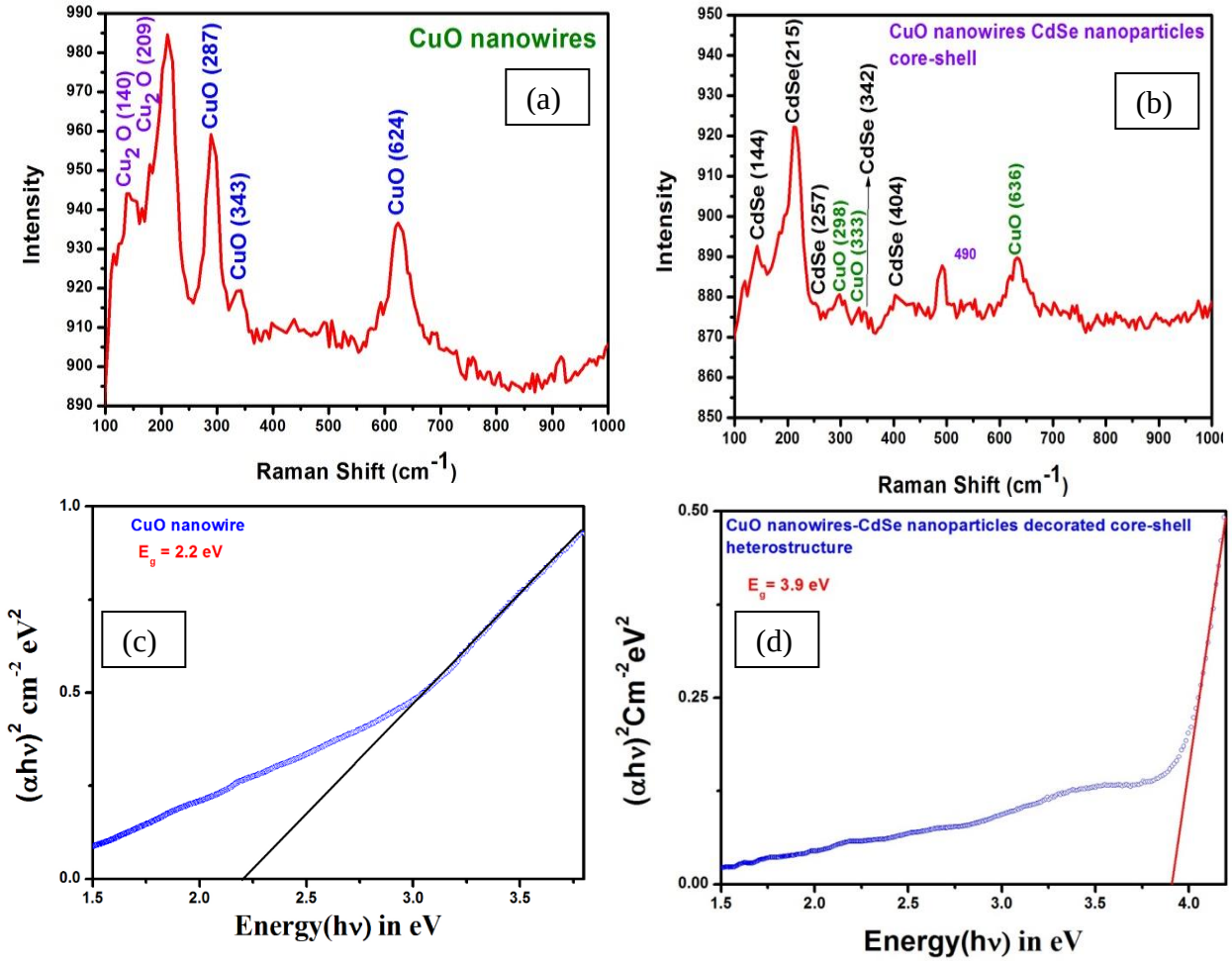

Figure 13: (a) Raman spectra of CuO nanowires which show three Raman active mode of vibration due to Cu-O stretching, (b) Raman spectra of CuO nanowires-CdSe nanoparticles decorated core-shell heterostructure in which CdSe vibration are also shown along with CuO three mode of vibration, (C) UV-Vis spectra of CuO nanowires, (d) UV-Vis of CuO-CdSe nanoparticles decorated core-shell heterostructure.

Figure 13(a) represents the Raman spectrum of CuO nanowires. The three strong peaks (287, 343 and 624 cm^{-1}) indicate the phonon modes in the CuO crystal corresponding to the Raman active modes of Ag, B*(g1)* and B*(g2)* symmetries. These peaks correspond to the

vibrations of the oxygen atoms. The Raman peaks at 140 cm^{-1} & 209 cm^{-1} correspond to Cu_2O. Raman spectrum of CuO-CdSe nanoparticles decorated core-shell heterostructure is shown in **Figure 13 (b).** The presence of CdSe raman peaks at 144 cm^{-1}, 215 cm^{-1}, 257 cm^{-1}, 342 cm^{-1}, 404 cm^{-1}due to Cd-Se stretching along with CuO confirms the presence of CuO-CdSe core shell nanomaterials prepared by CVD [1-8].

The UV-Vis spectra for CuO nanowires & CuO-CdSe heterostructure has been plotted as per the given equation **(Figure 13 (c), (d))** [9-10].

$$(\alpha h\upsilon)^{1/n} = (E_g - h\upsilon)$$

Where α = Co-efficient of absorbance, h = Plank's constant, υ = Frequency of UV-Vis light, E_g = Band gap of the materials, n= Allowed transitions (n=1/2 for first direct allowed transition).

In order to do UV-Vis spectroscopy, the materials have been dispersed in ethanol. The material dispersed solution has been taken for UV-Vis characterization. Fitting the plot according to the above equation, the band gap for the CuO nanowires is found to be approximately 2.2eV. The increase in the bandgap attributes the quantum confinement of the particles in the nanowires. The band gap is further increased to 3.96eV in the case of CuO-CdSe nanoparticles decorated core-shell heterostructure which attributes the confinement of the particles in both core and shell in the heterostructure [9-10].

4.6 Summary

- The CuO nanowires-CdSe nanoparticles decorated core-shell heterostructure is successfully synthesized by using our fabricated CVD.
- The FESEM & TEM images confirm the formation of CuO-CdSe nanoparticles decorated core-shell heterostructure along with beaded CdSe attached to the nanowires.
- Furthermore, the formation of crystalline CuO-CdSe nanoparticles decorated core-shell heterostructure has been established by XRD, SAD pattern, HRTEM, and RAMAN spectra characterization.
- The optical band gap measured for CuO nanowires and CuO-CdSe nanoparticles decorated core-shell heterostructure by using UV-Vis is found to be 2.2 eV and 3.9 eV, respectively.

References

1. T. Yu, X Zhao, Z.X. Shen, Y.H. Wu, W.H. Su, **Journal of Crystal Growth, 2004, 268, 590.**
2. D. Li, J. Hu, R. Wu and J. G Lu, **Nanotechology, 2010, 21, 485502.**
3. J.X. Wang, X.W. Sun, Y. Yang, K.K. Kyaw, X.Y. Huang, J.Z. Yin, J. Wei, H.V. Demir, **Nanotechnology, 2011, 22, 325704.**
4. A. S. Zoolfakar, R. A. Rani, A. J. Morfa, A. P. O'Mullane, K. Kalantar-zadeh\ **J. Mater. Chem. C, 2014, 2, 5247.**
5. J. Chrzanowski, J.C. Irwin **Solid State Communications, 1989, 70, 11.**
6. P.H. Shih, C.L. Cheng and S. Yun Wu **Nano. Res. Lett. 2013, 8, 398.**
7. A. Guleria, A. K. Singh, M. C. Rath, S. K. Sarkar and S. Adhikari **Dalton Trans., 2014, 43, 11843.**
8. X. Wang, Y. Xu, R. Tong, X. Zhou, Q. Li, H. Wang, **Cryst Eng Comm, 2015, 17, 960.**
9. B. D. Viezbicke, S. Patel, B. E. Davis, D. P. Birnie **Phys. Status Solidi B, 2015, 252, No. 8, 1700.**
10. T. Hao; T. Fei; X. Juan; L. Sunqi; L. Na; Z. Yunxuan; C. Mindong **Scientific Reports, 2015, 5 , 7770.**

Chapter-V

Characterization of CuO-CdS Nanoparticles Decorated Core-Shell Heterostructure

5.1 Introduction

Like CuO-CdSe core-shell heterostructure in Chapter-IV, in this chapter CuO-CdS core-shell heterostructure has been characterized by field emission scanning electron microscopy (FESEM) for morphological study, EDS for compositional analysis, x-ray diffraction (XRD) for phase confirmation, transmission electron microscopy (TEM), Raman spectroscopy for structural properties and UV-Vis spectroscopy for optical properties.

5.2 Field Emission Electron Microscopy (FESEM) & Energy Dispersive Spectroscopy (EDS)

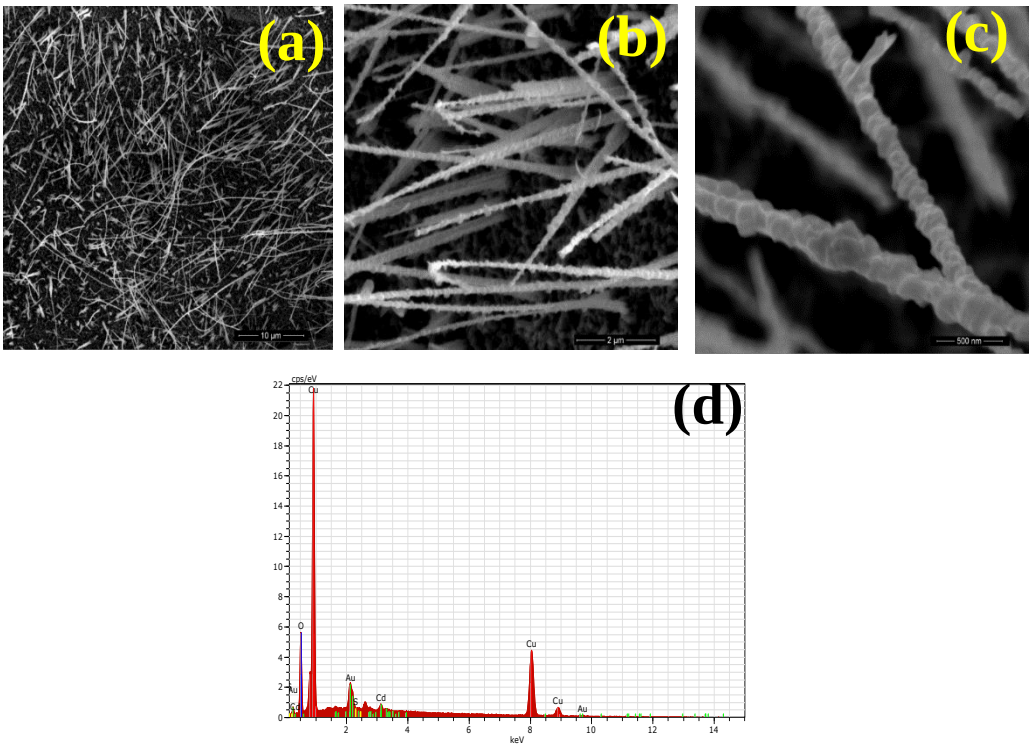

Figure 14: **(a) FESEM micrographs of CuO-CdS core-shell heterostructure synthesized by CVD technique (b), (c) Low & High-magnified image of CuO-CdS nanoparticles decorated core-shell heterostructure at scale bar 10μm & 500 nm, respectively; (d) EDS spectra for CuO-CdSe core-shell heterostructure**

The FESEM micrographs of nanoparticles decorated CuO-CdS core-shell heterostructure is shown in **Figure 14 (a)**. From the FESEM image it is to be noticed that the surface of CuO nanowires has been coated with CdS nanocrystallites completely thus forming a shell structure that has been confirmed by TEM and HRTEM. As observed by FESEM image **Figure 14(b)** the surface of CuO is smooth, however it has become rough by the coating of CdS nanocrystals onto the surface of CuO nanowires by CVD synthesis process. Change in thickness of the CuO-CdS core-shell nanowires as a whole has been observed and found to be ~0.195μm. This increase in the thickness is attributed to the deposition of CdS on CuO that forms CuO-CdS core-shell heterostructure during CVD process. The CuO-CdS heterostructures have grown along the length maintaining the original shape.

The elemental analysis of CuO-CdS has been carried out by EDS during FESEM investigation. The EDS spectra for CdS nanoparticles decorated CuO-CdS core-shell heterostructure is shown in **Figure 14(d)**. The existence of Cd, S, Cu, and O element confirm the heterostructure. The Spectra Au comes because Au particles are being coated before doing experiment.

5.3 X-ray Diffraction

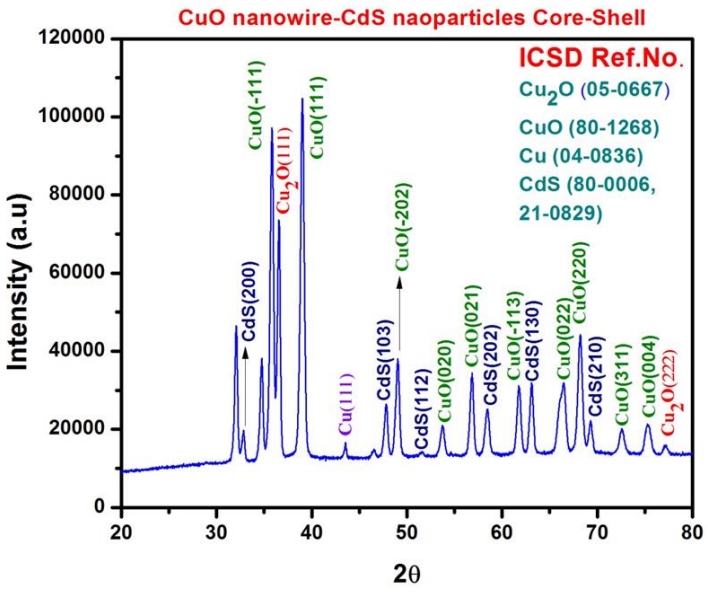

Figure 15: X-ray diffraction (XRD) pattern of CuO-CdS nanoparticles decorated core-shell heterostructure by using CVD technique.

The structural characteristics of the prepared material i.e. CuO-CdS core-shell heterostructure have been done by XRD. The XRD pattern of CdS nanoparticles coated CuO-CdS core-shell heterostructure is shown in **Figure 15**. The observed XRD patterns have been matched with the available standard data to conform about different phase of the prepared material. The pattern is well matched and indexed with the data ICDD No. - 80-0006(CdS), 05-0667(Cu2O), 80-1268(CuO), 04-0836(Cu). The matched peaks confirm the phase and crystalline nature of the material.

5.4 Transmission Electron Microscopy (TEM)

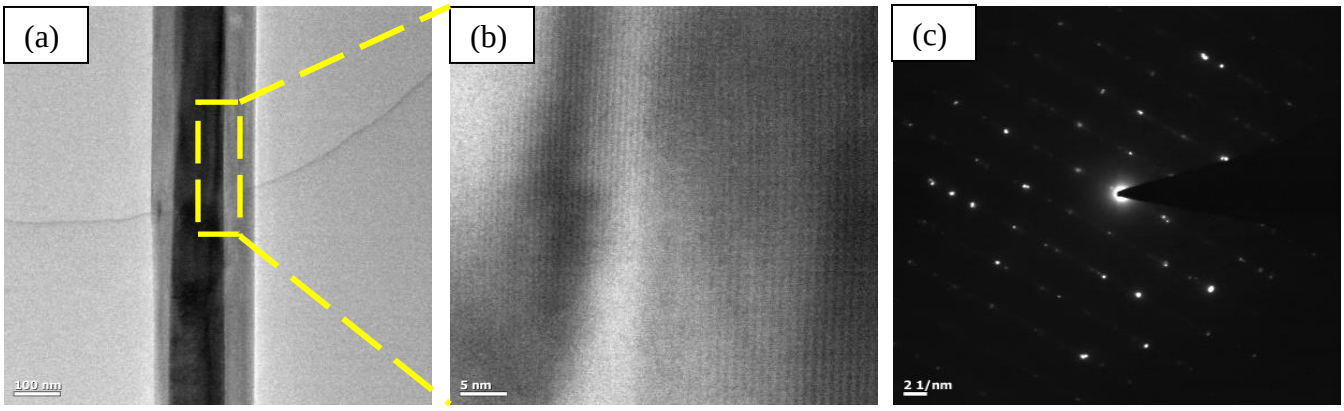

Figure 16: (a) TEM image of CuO-CdS nanoparticles decorated core-shell heterostructure which confirms the formation of core-shell heterostructure; (b) HRTEM of CuO-CdS nanoparticles decorated core-shell heterostructure; (d) SAED pattern of CuO-CdS nanoparticles decorated core-shell heterostructure.

The microstructure of CuO-CdS nanowires heterostructure has been investigated by using transmission electron microscopy (TEM) and high resolution transmission electron microscopy (HRTEM). The TEM image of CuO-CdS core-shell heterostructure is shown in **Figure 16(a)**. The TEM investigation shows forming CdS shell with CuO as core that forms CuO-CdS core shell structure. However, the surface seems to be smooth which is quite different structure as compared to the FESEM image of CuO-CdS heterostructure. It is believed that the loosely coated CdS nanoparticles must have detached from the surface during ultrasonication to prepare sample for TEM investigation. From the HRTEM image it could be noticed that the light dark part which is CuO that forms core and the over layer part is CdS that forms shell structure constituting a CuO-CdS core-Shell structure. The HRTEM image of CuO-CdS core-shell

heterostructure is shown in **Figure 16(b)**. The lattice fringe by HRTEM image reveals the crystalline nature of the CuO-CdS core-shell heterostructure. The directional matching of the lattice fringe suggest the probable epitaxial growth of CdS onto the surface of CuO nanowires. The SAED pattern further supports and confirms the crystalline nature of the materials (**Figure 16(c)**).

5.5 Raman Spectroscopy & UV-Vis Spectroscopy

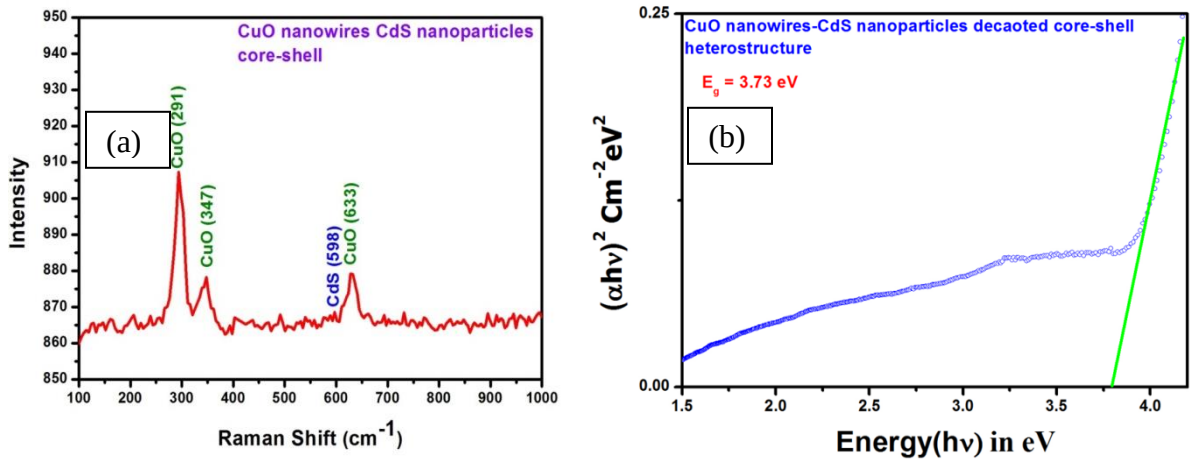

Figure 17: (a) Raman spectra of nanoparticles decorated CuO-CdS core-shell heterostructure in which CdS vibration is also shown along with CuO three mode of vibration; (b) UV-Vis of CuO-CdS nanoparticles decorated core-shell heterostructure.

Laser Raman spectroscopy is an important tool for studying materials because it provides information about the crystal structure and the presence of the disorder. Raman spectrum of CuO-CdS heterostructure is shown in **Figure 17(a)**. The observed peak around 598 cm^{-1} is attributed due to the Cd-S stretching mode of vibration. Other peaks around 287, 343 and 624 cm^{-1} belongs to the phonon modes in the CuO crystal corresponding to the three Raman active

modes of Ag, B *(g1)* and B *(g2)* symmetries. From the Raman spectra the presence of CdS on CuO is conformed [1-11].

The UV-Vis spectroscopy is a handy tool used to investigate the optical properties of the materials. The UV-Vis spectrum (Figure 17(b)) has been plotted according to the Tauc equation [12-15]

$$(\alpha h\upsilon)^{1/n} = (E_g - h\upsilon)$$

Where α = Co-efficient of absorbance, h = Plank's constant, υ = Frequency of UV-Vis light, E_g = Band gap of the materials, n= Allowed transitions (n=1/2 for first direct allowed transition).

The band gap for the CuO-CdS heterostructure is found to approximately 3.73eV. The increase in the bandgap is again inferred due to the quantum confinement of the particles in both core and shell in the heterostructure [12-15].

5.6 Summary

- Successfully prepared CuO-CdS core-shell heterostructure by using the self-fabricated CVD.
- The FESEM & TEM images confirm the formation of CuO-CdS core-shell heterostructure.
- Furthermore, the structural study of CdSe shell and crystalline nature of the materials is well supported by XRD, SAED pattern, HRTEM, and RAMAN spectra.
- The optical band gap for CuO nanowires and CuO-CdS core-shell heterostructure is found to be 2.2 eV and 3.73 eV, respectively.

References

1. K.K. Nanda, S.N. Sarangi, S.N. Sahu, S.K. Deb, S.N. Behera **Physica B., 1999, 262, 31.**
2. R.R. Prabhu, M.A. Khadar, **Bull. Mater. Sci., 2008, 31, 511.**
3. V.M. Dzhagan, M.Y. Valakh, C. Himcinschi, A. G. Milekhin, D. Solonenko, N. A. Yeryukov, O. E. Raevskaya, O. L. Stroyuk, D. R. T. Zahn, **J. Phys. Chem. C 2014, 118, 19492.**
4. T. Yu, X. Zhao, Z.X. Shen, Y.H. Wu, W.H .Su, **J. of Crys. Grow., 2004, 268, 590.**
5. D. Li, J, Hu, R. Wu, J. G. Lu, **Nanotechnology, 2010, 21, 485502.**
6. J.X. Wang, X.W. Sun, Y. Yang, K.K. Kyaw, X.Y. Huang, J.Z. Yin, J. Wei, H.V. Demir. **Nanotechnology, 2011, 22, 325704.**
7. A. S. Zoolfakar, R. A. Rani, A. J. Morfa, A. P. O'Mullaned, K. Kalantar-zadeh, **J. Mater. Chem. C., 2014, 2, 5247.**
8. J. Chrzanowski, J.C. Irwin **Solid Sta. Comm., 1989, 70, 11.**
9. P.H. Shih, C.L. Cheng, S. Y. Wu, **Nano. Res. Lett., 2013, 8, 398.**
10. A. Guleria, A. K. Singh, M. C. Rath, S. K. Sarkar, S. Adhikari, **Dalton Trans., 2014, 43, 11843.**
11. X. Wang, Y. Xu, R. Tong, X. Zhou, Q. Li, H. Wang, **Cryst Eng Comm., 2015, 17, 960.**

Chapter-VI

Growth Model & Current–Voltage Characteristics of CuO-CdX(X=Se, S) Nanoparticles Decorated Core-Shell Heterostructure

6.1 Introduction

Growth of low-dimensional heterostructures with modulated structures or compositions not only provides new systems to study fundamental physical properties at nanoscale but also exhibits technological importance for a variety of applications in nanoelectronics. However, the application largely depends on physical properties of prepared nanomaterials. The physical properties of the nanomaterials depend on the method of production—which controls, the size shape and crystallinity. Apart from that the physical properties of the nanomaterials also depends on growth mechanism [1]. Therefore, a thorough understanding of the growth mechanism may lead to large-scale and well-controlled synthetic process of nanomaterials. This process might provide the insight into the morphology-controllable design of high performance materials for nanodevices [2]. This chapter reviews the various core-shell hybrid nanostructures grown by the various techniques and their corresponding growth mechanisms. Jingjing et al. [3] have reported about the synthesis of **o**ne-dimensional Ag−Fe3O4 core−shell heteronanowires by co-precipitation method. In his work he has explained about the possible growth mechanism of core-shell occurs due to the concentration of reagent used. Zainelabdin et al. [4] have reported about th**e** hydrothermal synthesis of coral-like CuO nanostructures by selective growth on ZnO nanorods (NRs) at low temperatures. During the hydrothermal processing the resulting hydroxylated and eroded surface of ZnO NRs becomes favorable for the CuO nanostructures growth via oriented attachments. The synthesis of Cu/Cu2O/CuO core–shell nanowire heterostructures by combining a facile hydrothermal method and subsequent controlled oxidation process have been demonstrated by Zhao et al [5]**.** Guo et al [6] reported about the synthesis of ZnO/CuO Hetero-Hierarchical Nanotrees Array by hydrothermal route and discussed about the growth mechanism that relates the time of reaction and contact angle of droplet to the nanowires.

However, to best of our knowledge, so far there is no report about the CuO-CdSe and CuO-CdS prepared by CVD. Though there is no direct evidence to support , however, a probable growth mechanisms have been proposed, deduced from FESEM, high-resolution electron microscopy (HREM) images and existing report by other groups on heterostructures by CVD [2, 7-22]. The measured electrical behavior of the fabricated device under illumination is found to be photosensitive. This suggests that the heterostructure material in device structure could be used as potential photo detector application in future.

6.2 Growth Model

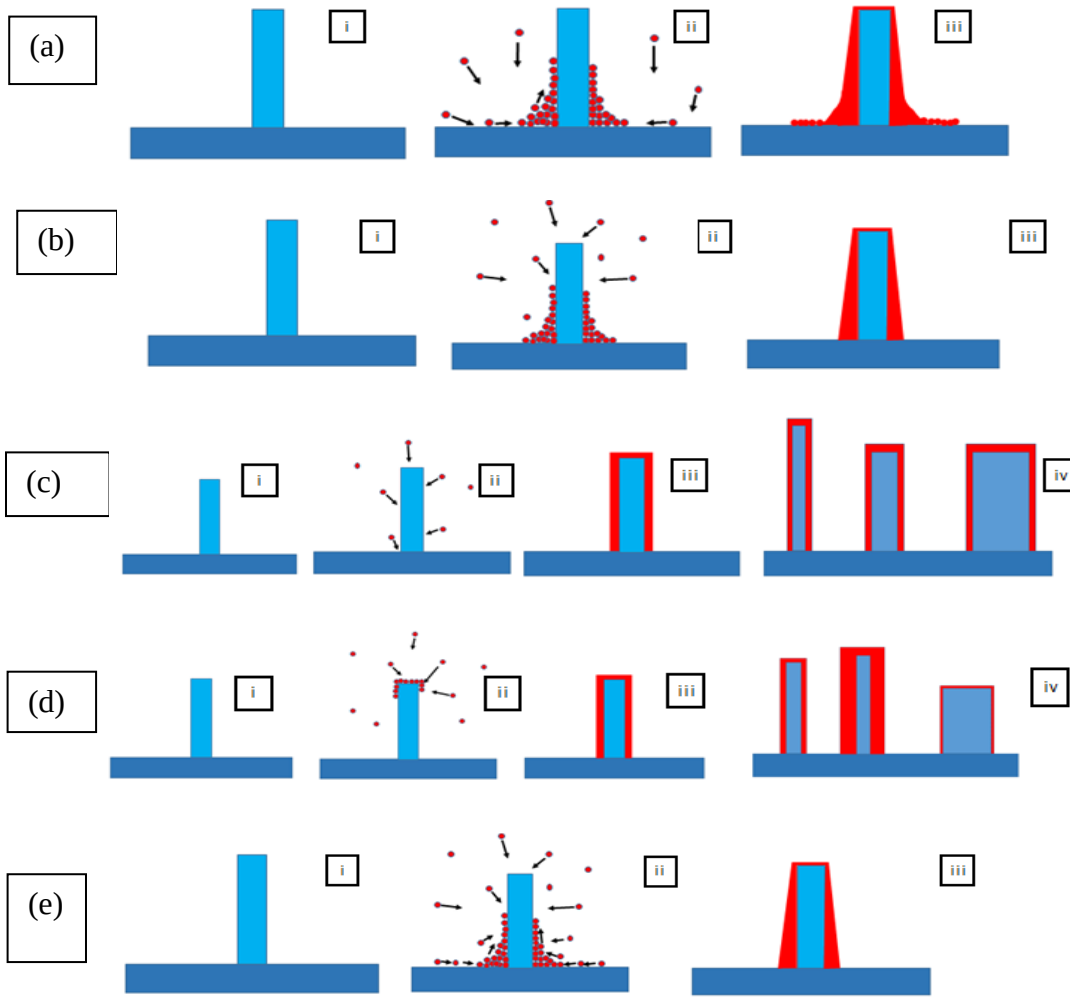

Figure 18: **Schematic illustration of the possible growth mechanism. Here, blue color corresponds to CuO nanowire; red color represents the CdSe molecules in vapor phase and subsequently forms a shell around the CuO nanowires (a) mass diffusion through the surface of nanowires, (b) Surface diffusion around the nanowires, (c) incorporation to the surface of nanowires, (d) transportation of particles across the length of the nanowires, (e) direct adsorption of particles onto the surface of nanowires**

Knowing the growth mechanism the produced objective heterostructure nanomaterials material could be tuned for desired applications in nanotechnology. Though much progress has been made in synthesis of hybrid nanostructured materials, the growth mechanism is not understood completely because the material product varies from run to run preparation condition. On this regard different suitable growth mechanism about heterostructures prepared by CVD has been proposed by various research groups all over the world. *Moore et al*. [2] have successfully prepared ultralong ZnS/SiO_2 core-shell nanowire by chemical vapor deposition (CVD). The formed single crystalline ZnS core with SiO_2 amorphous shell growth mechanism has highlighted various growth mechanisms. Their experimental investigations reveals about the volume and surface diffusion process of ZnS/SiO2 core-shell growth mechanism. *Person et al* [11] have reported that the growth of GaAs nanowires follows the Solid-phase diffusion mechanism rather than following general accepted theory of semiconductor nanowire growth i.e. vapor-liquid-solid (VLS) growth mechanism. The synthesis of Au particles assisted InAs nanowires by metallorganic vapor phase epitaxy (MOVPE) have been reported by *Kimberly et al.* [13]. In their work the failure of the VLS Mechanism in Au-Assisted MOVPE growth of InAs nanowires have been reported. Hence, this makes clear that the metal catalyst particle at the nanowire tip is no longer considered sufficient evidence to support the classic VLS formation process in whole or in part. *Gao et al.* [14] have reported about the crystallographic substrate orientation dependent growth of Sn catalyzed ZnO nanostructure. Furthermore, in another paper, he reported that the electronic properties of the substrate surface affect the growth of ZnO nanorods [15]. *Guozhang et al* [7] have reported about the one-step thermal evaporation process for the synthesis of Core/Shell CdSe/SiOx Nanowires. He has explained in his work regarding two stage growth mechanisms of the core/shell nanowires i.e. general VLS mechanism for the

growth of CdSe core by using metal catalyst and vapor-solid (VS) mechanism for the formation of SiOx shell. However, detailed growth mechanisms are missing in their reported. In the context of the growth mechanism of CuO-CdSe and CuO-CdS core-shell heterostructure nanomaterials referring to report by various research groups, some general trends have been identified. They are mass diffusion through the surface of nanowires, Surface diffusion around the nanowires, selective incorporation to the surface of nanowires, transportation of particles across the length of the nanowires and direct adsorption of particles onto the surface of nanowires could be possible growth mechanism of formation of core-shell heterostructure in these materials [2].

The growth mechanism illustrated schematically in **Figure 18(a)** demonstrates the mass diffusion through the surface of nanowires in which the nanowires (core) growth takes place along with shell formation originates through the surface of substrate, simultaneously. Synthesis via this mechanism is most likely to produce core-shell heterostructure that vary in thickness along the length. In short, we would expect to find variations in silica shell thickness along a single nanowire. This phenomenon would likely occur due to the increasing distance that the silica species would have to travel up the nanowire to reach close to the tip [10, 22].

A similar process is illustrated in **Figure 18(b**) in which surface diffusion around the nanowire occurs. In this case, the shell formation occurs via direct adsorption of gaseous particles. The bottoms of the core nanowires that have grown earliest are exposed to the gas phase particles for a longer period and, therefore form a thicker shell [10, 22].

Another possible synthesis route is presented **in Figure 18 (c)** which discusses about the incorporation of particles for the formation of core-shell structure. In this process, the core nanowires have formed first and then shell formation occurs. Previous reports have cited this

process as a possible formation mechanism for silica nanotubes in which the metal catalyst particle becomes completely encased. This type of mechanism would give core-shell heterostructure with completely uniform shell thickness, despite any variations in core size or structure, since at the time of shell formation the core would not be exhibiting dynamic growth as shown in figure part (v) [21].

Figure 18(d) reveals about the growth mechanism which involves transportation of particles across the length of the nanowires. In this case the shell formation originates on the tip of the nanowires to the bottom. Since the gas phase particles travels on the surface of the nanowire to the nanowire, it experiences a simultaneous and dynamic growth process. Variations in particle size and surface contact angle, among other factors, likely lead to observed thickness variations in the core and shell portions of our ultralong nanowires.

Figure 18(e) exhibits the growth mechanism in which the gas phase adsorption and surface diffusion of the particles simultaneously take place. In this case also, due to the surface diffusion of shell particles, the gaseous phase particles a dynamic nanowire which leads to the formation of various core-shell thicknesses [2].

The schematic illustration of gas phase adsorption growth mechanism of core-shell heterostructure is shown in **Figure 18(d).** In this growth mechanism, the particles are directly adsorbed on the surface of core materials from the gaseous phase leading to the formation of shell structure. Generally in this growth mechanism, uniform thickness of the core-shell heterostructure is maintained along the length(**Figure 18(d))**[2]. In the present work, the thickness of one dimensional CuO-CdSe is uniform throughout its length as observed from FESEM and HRTEM images. Hence the deduced experimental result suggests probable gas

phase adsorption growth mechanism in which CuO nanowires serves as template where CdSe particles are adsorbed from the vapor phase eventually forming one-dimensional CuO-CdSe core-shell heterostructure [7]. However, the exact growth mechanism is yet to be ascertained and needs further detail study.

The third possible growth mechanism is shown in **Figure 18(e)**, in which the formation of shell is due to simultaneous involvement of gas phase adsorption & surface diffusion mechanism for the formation of core-shell heterostcrture. As the surface diffusion of the particles takes place from the bottom, the gaseous particles experience a dynamic nanowires in which the gas phase adsorption of gaseous particles take place at different points of nanowires. As a result of which, the surface of the nanowires might be very rough and abrupt. However, the thickness might be different for different nanowires present in a single sample as it depends on various parameters like size of the gaseous particles; the surface contact angle will lead to the variation in shell thickness.

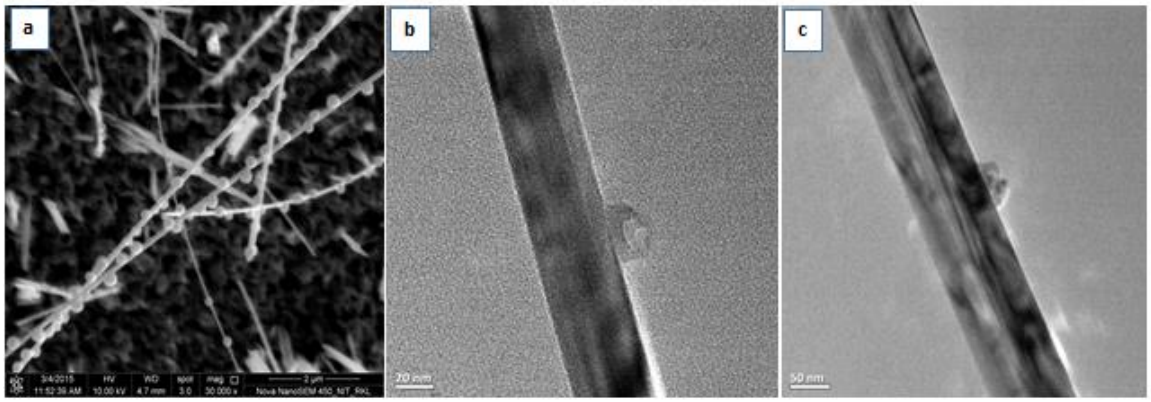

Figure 19: (a) FESEM Images of CuO-CdSe nanoparticles decorated core-shell heterostructure and (b), (c) TEM images of two nanowires that are prepared in same batch and same sample

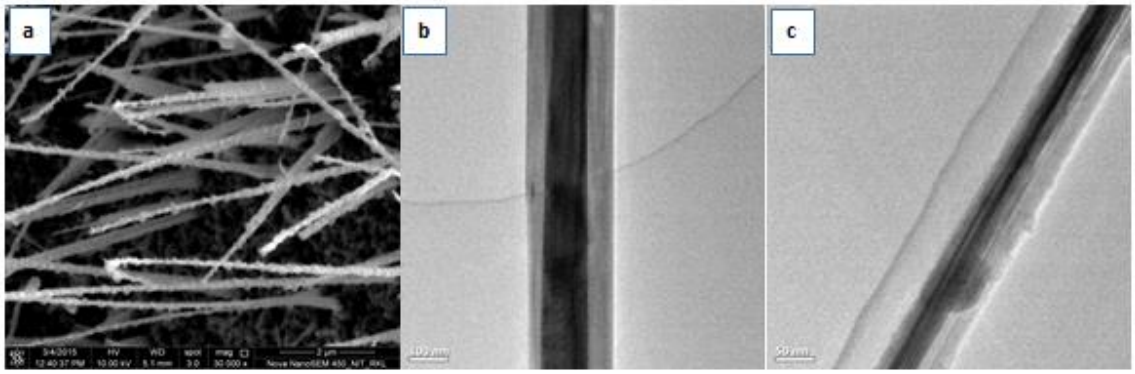

Figure 20: (a) FESEM Images of CuO-CdS nanoparticles decorated core-shell heterostructure and (b), (c) TEM images of two nanowires that are prepared in same batch and same sample.

The prepared core-shell heterostructure has been prepared by a different method and without using catalyst. The FESEM and HRTEM images reveal that the thickness of the CuO-CdS core-shell heterostructure is not uniform along its length. It is observed to be thicker at the bottom and gradually its thickness changes along the length. Therefore, based on experimental results and comparing with existing report, surface diffusion and gas phase adsorption probable growth mechanism of CuO-CdS is proposed. However, it needs further detail investigation to establish the exact growth mechanism.

6.3 Device Fabrication & Current-Voltage Characteristics of CuO-CdX (X=Se, S) Heterostructure

6.3.1 Device Fabrication for the Measurement of Current-Voltage Characteristics of Heterostructure under UV Illumination of 254 nm wavelength

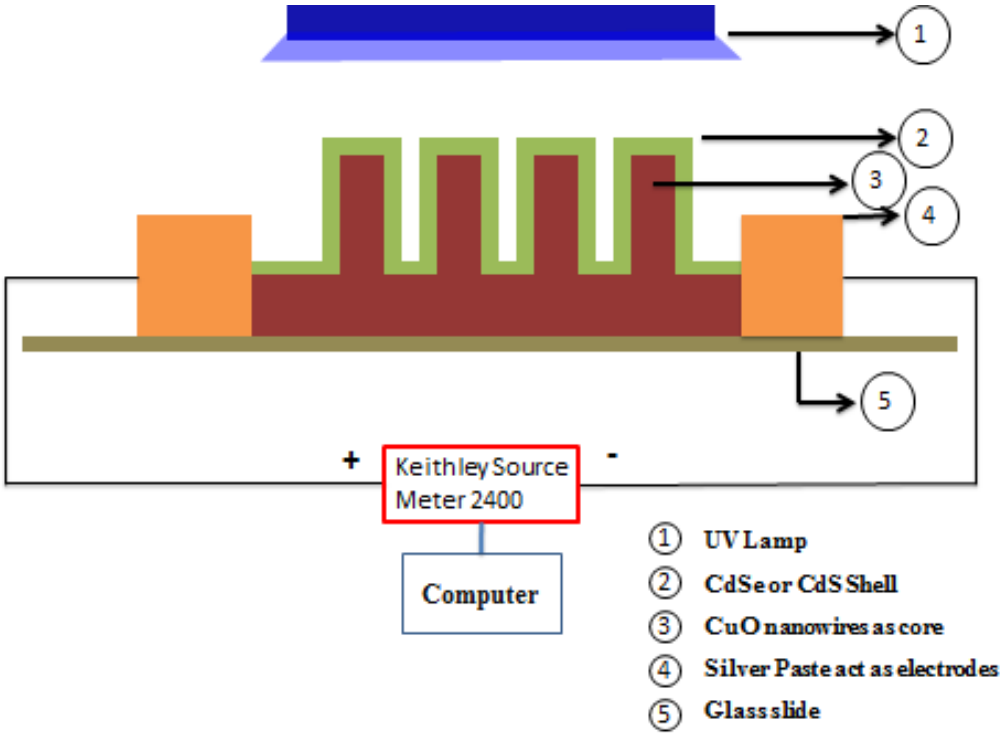

Figure 21: Device fabricated for the measurement of current-voltage of CuO nanowires, CuO-CdSe and CuO-CdS core-shell heterostructure in dark and under the illumination of UV light of wavelength 254 nm.

The architecture and fabrication of device for the measurement of current-voltage of CuO nanowires, CuO-CdSe and CuO-CdS core-shell heterostructure have been adopted from similar reported work [23, 24]. In order to fabricate the device for the measurement of current-voltage of CuO nanowires, CuO-CdSe and CuO-CdS core-shell heterostructure, a flake from each of the synthesized materials has been peeled off from the Cu substrate and laid onto the surface of a glass slide. Highly conducting silver paste has been used at the two opposite edges on the flake which act as electrodes. Very thin copper wires have been diffused into the silver point contact

and the other end has been connected to the source for supplying either voltage or current. Following same procedure electrical contacts have been made on CuO-CdX (X=Se, S) core-shell heterostructure. When the flake is peeled of a thing film of CuO is the base part of the material is exposed on which CdX (X=Se, S) has been grown. As shown in Figure, it is expected that the electrical contact is made on CuO and CuO-CdX. By supplying voltage from a source meter (Keithley Source Meter 2400) to the CuO-CdX device, output current has been measured. Current-voltage characteristics of the said device has also been measured under dark and illuminating light from a UV lamp.

6.3.2 Current-Voltage Characteristics of CuO-CdX (X=Se, S) under UV Illumination of 254 nm wavelength

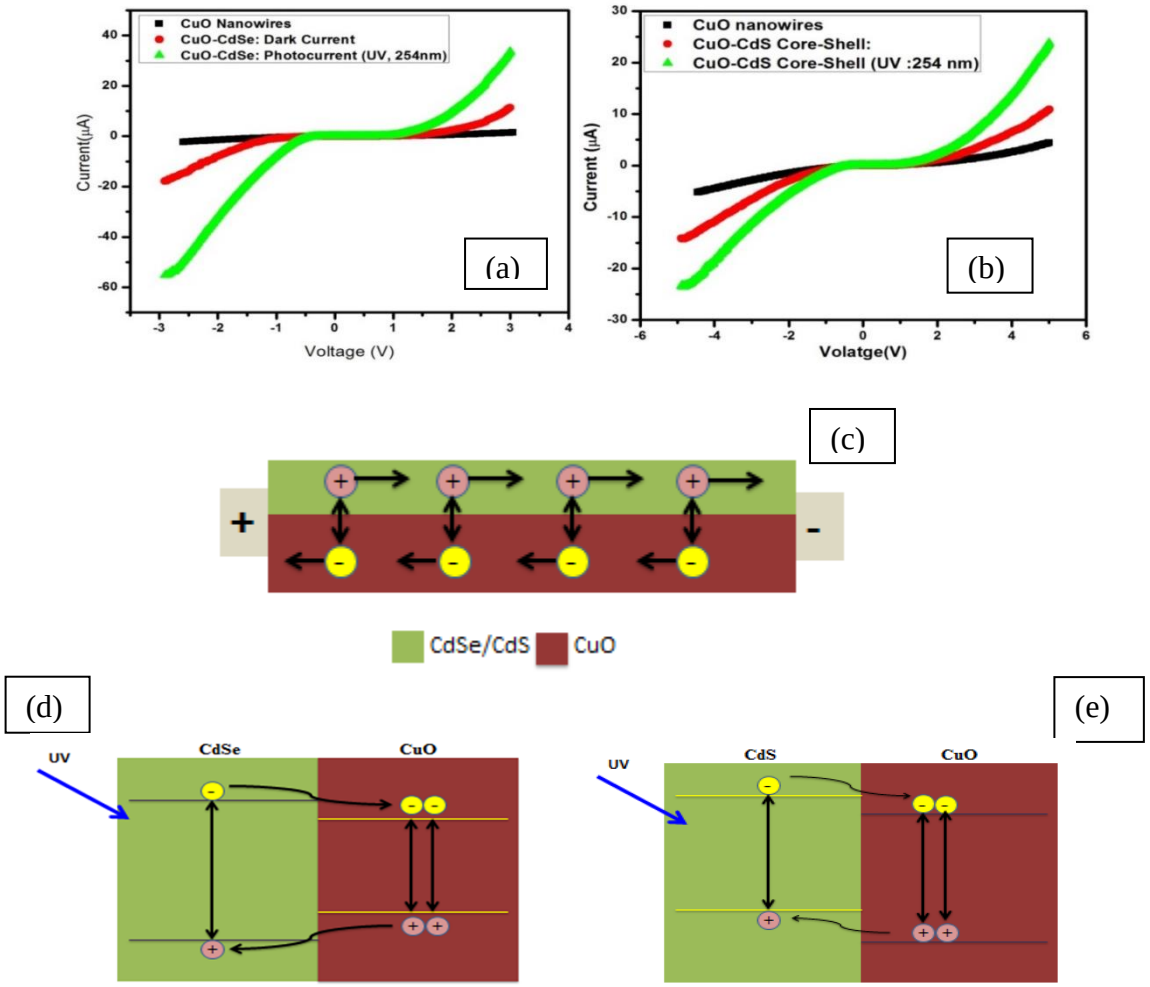

Figure 22: Current-Voltage Characteristics of (a) CuO nanowires & CuO-CdSe nanoparticles decorated core-shell heterostructure in dark & under UV illuminated; (b) CuO-CdS nanoparticles decorated core-shell heterostructure in dark & under UV illumination; (c) Animated diagram to show the charge transfer and separation of electron-hole under UV illumination; (d), (e) Schematic diagram of energy band structure (Type-I band alignment), in the CuO-CdSe heterostructure & (Type-II band alignment) CuO-CdS heterostructure under UV light illumination of 254 nm wavelength [9].

The current (I)-voltage (V) characteristics of the CuO nanowires, CuO-CdSe and CuO-CdS heterostructure in dark & under illumination (254 nm) have been done separately. The I-V characteristics of CuO-CdSe core-shell heterostructure has been measured at biasing voltage 3V. The I-V of CuO nanowires and CuO-CdSe core-shell heterostructure has been plotted in a single graph in order to see the change in current in the materials as shown in **Figure 22(a)**. The maximum current for CuO nanowires is found to be 1.4 µA. The dark-current is found to be 11µA for CuO-CdSe core-shell heterostcrture. The photo-current is found to be 33µA for CuO-CdSe core-shell heterostcrture when measured under UV illumination of wavelength 254 nm.

Similarly, the I-V characteristics for CuO-CdS core-shell heterostructure have been measured at biasing 5V. The I-V graph for CuO nanowires and CuO-CdS core-shell heterostructure has been plotted in a single work sheet to check the change in current in the materials as shown in **Figure 22(b).** The current for CuO nanowires is found to be 4.4µA at 5V biasing. The dark-current is further found to 10.8µA for CuO-CdS core-shell heterostructure. The photo-current is found to be increased to 23.8µA for CuO-CdS corer-shell heterostructure when illuminated by UV light of wavelength 254 nm. The reason behind applying two different voltages is that while taking measurement at 5V, the device CuO-CdSe degrades due resistive heating in core-shell heterostcrture at this voltage.

It has been observed from the both characteristics graph **(Figure 22(a) & 22(b))** that there is a significant change in dark current of CdX(X=Se, S) as compared to the dark current of CuO nanowires, which may be due the enhancement in charge carriers by decorating CdSe or CdS nanoparticles onto the surface of CuO nanowires. When the UV light (wavelength=254 nm) is illuminated on CuO-CdSe, CuO-CdS fabricated device, increase in photo-current is observed as compared to dark current for both the respective heterostructures. The increase in photocurrent

in the materials is attributed due to the effective charge separation as shown in **Figure 22 (c)** of the photo-generated electron and holes under UV illumination [25-27]. Since the illuminated UV radiation is having high energy than CuO & CdSe or CdS, both core and shell of the heterostructure of the materials is excited and give rise to photo-induced electrons [28]. It should be noted that this dramatic improvement in photocurrent indicates that the recombination of photo-generated electrons is effectively inhibited due to the formation of the core/shell heterojunction structure. Similar results haven reported by other group [29].

Figure 22 (d), (e) shows the type-I and type-II band alignment of CuO-CdSe and CuO-CdS heterostructure, respectively. When the material is under illumination, the electron of CuO and CdSe/CdS present in their respective valence band are excited and move to their respective conduction band. The photo-generated electrons in the conduction band of CdSe or CdS are injected to the conduction band of CuO, leading to the high electron concentration in the conduction band of CuO. Due to the high carrier mobility, the high-crystalline CuO core makes it an effective channel for conducting electrons, while the holes are transported through CdSe/CdS. The separation of the charge carrier types minimizes their recombination rate, thus, increasing the photocurrent [29-31].

6.4 Summary

- Based on experimental investigation and comparing the existing report, gas phase adsorption growth mechanism for CuO-CdSe core-shell heterostructure have been proposed.
- Similarly, for the CuO-CdS core-shell heterostructure, the probable growth mechanism is surface diffusion and gas phase adsorption has been attributed.
- The current is found to be dramatically increased in heterostructures and further increase in current is due to illumination of high energy UV light.
- The current of CuO-CdSe is increased to 11µA from 4.4µA (CuO nanowire)
- The current of CuO-CdSe is increased further from 11µA to 33µA when illuminated by UV light (254 nm)
- The current of CuO-CdS is increased to 10.8µA from 4.4µA (CuO nanowire)
- The current of CuO-CdS is increased further from 10.8µA to 23.8µA when illuminated by UV light (254 nm)

References

1. F. Wang, Z. Yang, S. Yip, G. Dong, Jared J. Hou, Y. Chueh, Johnny C. Ho, **J. Nanomater., 2014, 14, 702859.**
2. D. Moore, J. R. Morber, R. L. Snyder, and Z. L. Wang, **J. Phys. Chem. C 2008, 112, 2895.**
3. J. Ma, K. Wang, and M. Zhan, **ACS Appl. Mater. Interfaces, 2015, 7, 16027.**
4. A. Zainelabdin, G. Amin, S. Zaman, O. Nur, J. Lu, L. Hultman and M. Willander **J.Mater. Chem., 2012, 22, 11583.**
5. Y. Zhao, Y. Zhang, H. Zhao, Y. Li, L. Wen, Z. Yan, Z. Huo, **Nano Res., 2015, 8, 2763.**
6. Z. Guo , X. Chen , J. Li , J.H. Liu, and X.J. Huang, **Langmuir 2011, 27, 6193.**
7. G. Dai, S. Yang, M. Yan, Q. Wan, Q. Zhang, A. Pan, B. Zou **J. Nanomater., 2010, 427689, 6.**
8. Y.Y. Choi, S. J. Parka, D. J. Choi, **Cryst Eng Comm, 2012, 14, 1737.**
9. Y. Yoshida, K. Uto, M. Hattori and M. Tsuji, **Cryst Eng Comm, 2014, 16, 5672.**
10. E.I. Givargizov, **J. Cryst Growth 1975, 31, 20.**
11. A. I. Persson, M. W. Larsson, S. Stenström, B. J. Ohlsson, L. Samuelson, L. R. Wallenberg, **Nat. Mater. 2004, 3, 677.**
12. M. Leone, S. Agnello, R. Boscaino, M. Cannas, F. M. Gelardi, **Phys. ReV. B 1999, 60, 11475.**
13. K. A. Dick , K. Deppert , T. Mårtensson , B. Mandl , L. Samuelson , W. Seifert , **Nano Lett. 2005, 5, 761.**
14. P. X. Gao, Y. Ding , and Z. L. Wang , **Nano Lett. 2003, 3, 1315.**
15. P. X. Gao, Z. L. Wang, **J. Phys. Chem. B 2004, 108, 7534.**

16. S. Kodambaka, J. Tersoff, M. C. Reuter, F. M, Ross, **Phys. ReV. Lett. 2006, 96.**

17. J. D. Holmes, K. P. Johnston, R. C. Doty, B. A.Korgel, **Science. 2000, 287, 1471.**

18. J. Westwater, D. P. Gosain, S. Usui, **Phys. Status Solidi A 1998, 165, 37.**

19. S. J. Kwon, J.G. Park, **J. Phys.: Condens. Matter 2006, 18, 3875.**

20. E. L. Cussler and Frontmatter, **Diffusion: mass transfer in fluid systems, 2nd ed.; Cambridge University Press: New York, 1997.**

21. H. Wang, G. S. Fischman, **J. Appl. Phys. 1994, 76, 1557.**

22. Y. Wang, V. Schmidt, S. Senz, U. Gösele, **Nat. Nanotechnol. 2006, 1, 186.**

23. A A El Mel, M. Buffière, N. Bouts, E. Gautron, P. Y. Tessier, K. Henzler, P. Guttmann, S. Konstantinidis, C. Bittencourt, R. Snyders, **Nanotechnology, 2013, 24 265603.**

24. T. Song, S.T. Lee, B. Sun, **J. Mater. Chem., 2012, 22, 4216.**

25. C.H. Lin, T.T. Chen, Y.F. Chen, **Opt. Express, 2008, 16, 16916.**

26. R. Chakraborty, F. Greullet, C. George, D. Baranov, E. D. Fabrizio, R. Krahne, **Nanoscale, 2013, 5, 5334.**

27. A. Persano, A. Taurino, P. Prete, N. Lovergine, B. Nabet, A. Cola, **Nanotechnology, 2012, 23, 465701.**

28. F. Zhang, Y. Ding, Y. Zhang, X. Zhang, Z.L Wang, ***ACS Nano*, 2012, 6,10, 9229.**

29. H. Wang, L. Zhang, Z. Chen, J. Hu, S. Li, Z. Wang, J. Liu, X. Wang, **Chem. Soc. Rev., 2014, 43, 5234.**

30. Z. Yang, L. Guo, B. Zu, Y. Guo, T. Xu, X. Dou, **Adv. Optical Mater. 2014, 2, 738.**

31. X. Wang, H. Zhu, Y. Xu, H. Wang, Y. Tao, S. Hark, X. Xiao, Q. Li, **ACS Nano, 2010, 4, 3302.**

Chapter-VII

Conclusion & Future Research Scope

7.1 Conclusion

A low cost CVD setup has been fabricated successfully. Using the self-fabricated CVD, the CuO nanowires-CdX (X= Se, S) nanoparticles decorated core-shell heterostructure has been synthesized successfully. The synthesized materials have been characterized by FESEM, XRD, TEM, HRTEM, SAED, Raman spectroscopy, UV-Vis spectroscopy. The FESEM image of CuO nanowires reveals the formation of dense nanowires grown all over the places having high aspect ratio. Furthermore, the formation of core-shell structure is well confirmed by the TEM and HRTEM images.

The formation of the beaded structure of CdSe onto the surface CuO-CdSe heterostructure has been obtained by CVD. XRD pattern confirms the presence highly crystalline nature of CdSe phase in the sample along with CuO, Cu_2O & Cu phase. The structure and crystalline nature of the heterostructure is further ascertained by TEM, HRTEM, and SAED characterization. The RAMAN spectroscopy of CuO-CdSe heterostructure confirms the presence of CdSe in the material. The band gap measured for CuO nanowires and CuO-CdSe heterostructure using UV-Vis spectra is found to be ~2.2eV & ~3.96eV, respectively.

Similarly, formation of CuO-CdS core-shell heterostructure have been also obtained by self-fabricated CVD process, which has been confirmed observing the morphology by FESEM. The XRD, TEM, HRTEM and SAED characterization confirms the formation crystalline nature of CuO-CdS core-shell heterostructure. The RAMAN spectroscopy confirms the presence CdS in the material. The band gap is found to be ~3.73eV as observed by UV-Vis spectroscopy.

Furthermore, the growth model for the synthesis of core-shell heterostructure has been discussed. Gas phase interaction of CdSe gaseous particle with the CuO nanowires surface leads

to the formation of CuO-CdSe heterostructure suggests gas phase adsorption growth mechanism For CuO-CdS surface diffusion & gas phase interaction has been suggested as possible growth mechanism. The synthesized heterostructure have been fabricated into a device for the measurement of current-voltage characteristics in dark and under the illumination of UV light of 254nm wavelength. The dark current at biasing 3V for CuO nanowires is found to be 1.4μA. The current is further increased to 11μA and 10.8μA in heterostructure for CuO-CdSe & CuO-CdS, respectively. When illuminated by UV, the photocurrent is further increased to 33μA & 23.8μA for CuO-CdSe & CuO-CdS heterostructure, respectively. This investigation reveals that the material device could be use as probable photo detector in future.

7.2 Future Research Scope

Since, CuO-CdSe & CuO-CdS heterostructure are a new class of hybrid nanomaterials, the research in this system is wide open. The future research scopes in this field are given below.

1. To investigate further the quantitative analysis of the growth of CuO-CdSe & CuO-CdS heterostructure in detail.

2. To study various applications such as gas sensors, photodetector based on single core-shell heterostructure of CuO-CdSe and CuO-CdS.

3. To study the field emission properties of CuO-CdSe & CuO-CdS heterostructure.

4. To investigate the heterostructures for solar cell application and other energy related applications.

5. To investigate the influence of electric field during the growth of heterostructure using two electrodes that has been fitted at the downstream of the CVD.

APPENDIX

Appendix-1

Equipment Used

Sl No.	Name of The Instrument	Model name & Specification
1	X- ray diffraction	RIGAKU JAPAN/ULTIMA-IV Wavelength of X-Ray: $\lambda = 1.5406A^0$ Target Cu K_α, $\lambda = 1.5406A^0$
2	Field Emission Scanning Electron Microscope	Nova Nano SEM/ FEI Signals: BSE(Back Scattered Electron) SE(Secondary) X-ray for EDS (electron Dispersive Spectroscopy)
3	Transmission Electron Microscopy (TEM)	TECNAI 92 F20 ST Energy: 200kV
4	Raman Spectroscopy	Thermo-Nicolet 6700
5	UV-Vis Spectroscopy	Lambda 35, Perkin Elmer Scanning range: 200nm-1000nm
6	Ultrasonicator	LABMAN LMUC Series
7	I-V measurement	Keithley source meter model 2400 Source voltage: 5µV-210V Source current:50pA-1.05A Measure voltage: 1µV-211V Measure current:10pA-1.055A Measure resistance: 100µΩ-211MΩ
8	three zone horizontal furnace	Lenton furnace Heating zone: 70 cm Heating element: Silicon carbide Maximum Temperature: from 100-1500^{0}C

BIO-DATA

Mr. Bamadev Das was born on 23rd February 1990, hailing from the picturesque land of Odisha, India. He received his B. Sc. (Physics) in 2010 from Rairangpur College, Rairangpur, (North Odisha University) and M. Sc. degrees in Physics from National Institute of Technology (NIT) Rourkela in 2012. He has joined Master of Technology (Research) in Physics at Department of Physics & Astronomy in National Institute of Technology Rourkela. His current research interests include chemical vapor deposition (CVD), nanomaterials, hybrid nanomaterials, carbon nanotubes (CNT), and graphene.